

1
2
3 **Advances in Bioengineering Pancreatic**
4 **Tumor-Stroma Physiometric Biomodels**

5
6
7 Maria V. Monteiro[#], Luís P. Ferreira[#], Marta Rocha, Vítor M. Gaspar* and João F.
8 Mano*

9
10
11 Department of Chemistry, CICECO, University of Aveiro, Campus Universitário de
12 Santiago, 3810-193, Aveiro, Portugal

13
14
15 #Authors contributed equally

16 *Corresponding authors:

17 Dr. Vítor Gaspar and Professor João Mano

18 Department of Chemistry, CICECO – Aveiro Institute of Materials

19 University of Aveiro, Campus Universitário de Santiago

20 3810-193, Aveiro, Portugal

21 E-mail: vm.gaspar@ua.pt, jmano@ua.pt

22 Telephone: +351 234370733

23 **Abstract**

24 Pancreatic cancer exhibits a unique bioarchitecture and desmoplastic cancer-stroma interplay
25 that governs disease progression, multi-resistance, and metastasis. Emulating the biological
26 features and microenvironment heterogeneity of pancreatic cancer stroma *in vitro* is
27 remarkably complex, yet highly desirable for advancing the discovery of innovative
28 therapeutics. Diverse bioengineering approaches exploiting patient-derived organoids,
29 cancer-on-a-chip platforms, and 3D bioprinted living constructs have been rapidly emerging
30 in an endeavor to seamlessly recapitulate major cancer-stroma biodynamic interactions in a
31 preclinical setting. Gathering on this, herein we showcase and discuss the most recent
32 advances in bio-assembling pancreatic tumor-stroma models that mimic key disease
33 hallmarks and the native desmoplastic biosignature. A reverse engineering perspective of
34 pancreatic tumor-stroma key elementary units is also provided and complemented by a
35 detailed description of biodesign guidelines that are to be considered for improving 3D
36 models physiomimetic features. This overview provides valuable examples and starting
37 guidelines for researchers envisioning to engineer and characterize stroma-rich biomimetic
38 tumor models. All in all, leveraging advanced bioengineering tools for capturing stromal
39 heterogeneity and dynamics, opens new avenues toward generating more predictive and
40 patient-personalized organotypic 3D *in vitro* platforms for screening transformative
41 therapeutics targeting tumor stroma.

42

43 **Keywords:** Pancreatic Tumor-Stroma, *In Vitro* Models, Organoids, 3D Bioprinting, Cancer-
44 on-a-chip

45

46 1. Introduction

47 Pancreatic cancer is a highly lethal malignancy that is becoming increasingly prevalent
48 worldwide.(Makohon-Moore and Iacobuzio-Donahue, 2016) Among all types of pancreatic
49 cancer sub-types identified to date, pancreatic ductal adenocarcinoma (PDAC) is the most
50 prevalent and the most challenging to tackle clinically, exhibiting a 5-year survival rate of
51 approximately 8%.(Kuen et al., 2017; Orth et al., 2019) The poor prognosis of this neoplasia
52 is intimately correlated with the unique bioarchitecture of its stromal components.(Gaviraghi
53 et al., 2011; Pandol et al., 2009) Indeed, mounting evidence regarding PDAC tumor
54 microenvironment (TME) indicate that its highly heterogeneous and desmoplastic
55 distal/juxtatumoral stroma is a key effector in disease progression.(Schnittert et al., 2019;
56 Weniger et al., 2018) In PDAC, the stromal compartment is particularly prevalent and
57 bioactive having a major role in disease progression and drug resistance when compared to
58 those of other solid tumors.(Kleeff et al., 2016) In this intricate setting, tumor-associated
59 stromal elements actively communicate with their surrounding microenvironment and
60 specifically with pancreatic cancer cells via numerous routes significantly modulating gene
61 expression patterns, metabolic signatures, invasion/metastasis and resistance mechanisms
62 activation.(Zhan et al., 2017) Improving our understanding and recapitulation of such
63 multifactorial cancer-stromal interactions is crucial for discovering innovative biological
64 targets.

65 Up-to-date, remarkable efforts and advances have been made toward generating
66 increasingly physiomimetic 3D *in vitro* models that can more accurately recapitulate the
67 biological and biophysical complexity of the TME. Such living 3D models greatly surpass
68 the limitations of 2D monolayered cell cultures and the costly/low-throughput animal models
69 which generally fall short in recapitulating the heterogeneous and highly fibrotic stroma
70 components of PDAC.(Fang and Eglen, 2017; Laschke and Menger, 2017) The available
71 toolbox of bioengineered 3D models for mimicking human disease in an *in vitro* setting
72 includes: (i) cell-rich randomly assembled 3D spheroids, (ii) patient-derived organoids, (iii)
73 cell-laden hydrogel platforms, (iv) dynamic microfluidics-based cancer-on-a-chip platforms,
74 as well as 3D biofabricated constructs, and/or their combinations thereof.(Baker et al., 2016;
75 Cao et al., 2019a; Ferreira et al., 2021; Huang et al., 2015; M. V. Monteiro et al., 2020a; Yu
76 and Choudhury, 2019) In effect, evermore organotypic patient-derived organoids combined
77 with microfluidic chips and 3D additive manufacturing living constructs are rapidly
78 emerging as proficient platforms for recapitulating key aspects of the TME.(Monteiro et al.,
79 2021b) Such capacity to mimic critical flow dynamics, as well as the biochemical, genetic,
80 and biophysical cues that underly cancer progression are expected to contribute for unveiling
81 critical aspects that ultimately influence therapeutics efficacy evaluation.(Cao et al., 2019b;
82 Li et al., 2019; Zhang et al., 2017) In many ways these rapidly emerging platforms have also
83 potential for transforming the foundations of the field of preclinical cancer modelling owing
84 to their inherent modularity and bioengineering versatility, offering researchers the
85 possibility for precisely introducing key TME elements and tumor tissue-stroma dynamics
86 that are still challenging to be recapitulated *in vitro*. Achieving the successful inclusion of
87 key stromal cellular effectors, and of the supporting pancreatic cancer ECM matrix, in a
88 mode that recapitulates patient tumor cellular landscape, disease stage and desmoplastic
89 environment, is anticipated to provide significant breakthroughs.

90 Gathering on the relevance of mimicking tumor-stroma interactions in *in vitro* models,
91 herein we showcase and critically discuss the most recent and significant advances in
92 exploring 3D platforms for modeling the unique PDAC tumor-stroma interplay. A
93 comprehensive overview of key design blueprints for bioengineering stroma-rich p models is

94 also provided in light of the key unitary elements and analytical tools that can be used to
95 intelligently generate physiomimetic living systems for better predicting candidate
96 therapeutics performance before their translation to a clinical setting.

97 98 **2. Pancreatic Tumor – Stromal Cells Interplay – An Undesirable Alliance**

99 Pancreatic tumors stroma is unique in comparison to other malignancies in the sense that
100 stromal constituents provide key signaling and bioprotective barriers that fuel disease
101 progression and protect cancer cells from anti-cancer therapeutics.(Ho et al., 2020) In a
102 bottom-up deconstructive perspective, PDAC stroma consists of key fundamental building
103 blocks and core effectors including: (i) cancer-associated fibroblasts (CAFs), (ii) endothelial
104 cells, (iii) immune system cells (*e.g.*, TAMs, Myeloid-derived suppressor cells (MDSCs),
105 etc.), alongside with basement membrane and extracellular matrix (ECM)
106 components.(Pothula et al., 2020; Stopa et al., 2020) Pancreatic tumors also actively
107 influence surrounding lymphatic and autonomic nervous system elements, through direct
108 and indirect means of communication using soluble/insoluble biomolecular mediators (*e.g.*,
109 growth factors, cytokines, extracellular vesicles).(Tomás-Bort et al., 2020)

110 Up-to-date highly relevant clinical findings have highlighted that CAFs play an essential
111 part in establishing the fibrotic stromal barrier that engulfs the tumor mass, and that
112 ultimately impedes therapeutics access.(Grünwald et al., 2021) In PDAC, cancer-associated
113 pancreatic stellate cells (CAFs) assemble in a core-shell like structure with distinct cellular
114 and matrix composition surrounding the primary tumor site.(Grünwald et al., 2021; Sun et
115 al., 2018) CAFs have been hypothesized to arise from pancreatic stellate cells (PaSCs).(Apte
116 et al., 2013) In healthy tissues PaSCs exhibit a star-shaped morphology, recognized by the
117 expression of both ectodermal and mesenchymal markers and by their capacity to store key
118 retinoids such as vitamin A-rich in lipid droplets.(Pothula et al., 2020; Schnittert et al., 2019)
119 While PaSCs have been speculated to play a minor role as regulators of pancreatic acinar
120 secretions and of localized immune response, these cells are well recognized as crucial
121 mediators of pancreatic ECM function.(Ferdek and Jakubowska, 2017; Suklabaidya et al.,
122 2018) During PDAC development, PaSCs found in the periacinar region, can be activated in
123 response to inflammatory cues and cancer cells-derived factors, acquiring a myofibroblast
124 phenotype capable of deregulating ECM homeostasis, and also actively interfere with
125 immune cell response (Wang et al., 2020). Generally, PaSCs transformation to CAFs is
126 expedited by cancer cells-mediated secretion of growth factor β (TGF- β), tumor necrosis
127 factor α (TNF- α), platelet-derived growth factor (PDGF), and several interleukins (*e.g.*, IL-
128 1, -6, and -10).(Bynigeri et al., 2017)

129 Once transformed, CAFs establish complex a complex autocrine and paracrine signaling
130 interplay with cancer cells, by secreting increased levels of cytokines (*e.g.*, IL-1, -6, -8 and
131 -10) and growth factors (*e.g.*, transforming growth factor β (TGF- β), insulin-like growth
132 factor 1 (IGF-1), vascular endothelial growth factor (VEGF), platelet-derived growth factor
133 (PDGF), fibroblast growth factor 2 (FGF-2), connective growth factor (CTGF), and C-X-C
134 motif chemokine 12 (CXCL12).(Norton et al., 2020; Sun et al., 2018) All these soluble
135 molecules contribute to the desmoplastic reaction and promote cancer cells proliferation,
136 migration, invasion, and resistance.(Hosein et al., 2020) On the other hand, CAFs also
137 exhibit an important role on cancer cells metabolic reprogramming by providing necessary
138 biomolecular cues that support cancer survival under nutrient-deprived
139 conditions.(Schnittert et al., 2019)

140 In this biodynamic microenvironment, CAFs are in turn stimulated by cancer cell-derived
141 mediators such as hepatocyte growth factor (HGF) and fibroblast growth factor

142 (FGF)(Pereira et al., 2019), leading to increased matrix deposition and remodeling.(Luo et
143 al., 2012) Such interplay further promotes tumor hypoxia, and surrounding blood vessels
144 collapse, promoting epithelial-to-mesenchymal transition (EMT), increased cancer cells
145 malignant behavior, and hampering anti-cancer therapeutics delivery and
146 performance.(Kleeff et al., 2007; Sahai et al., 2020) More importantly, CAFs also exhibit
147 extensive reciprocal signaling with TME infiltrating immune cells.(Watt and Kocher, 2013)
148 This direct contact with cancer cells and crosstalk with immune cells is hypothesized to
149 further increase pancreatic cancers ability to evade immune response.(Bynigeri et al., 2017;
150 Norton et al., 2020)

151 Adding to this, pancreatic stroma is also populated by a complex immune cell niche. The
152 immune compartment is rich in effector T cells, NK cells, and macrophages, which in all are
153 counteracted by competing immunosuppressive tumor-associated macrophages (TAMs),
154 myeloid-derived suppressor cells (MDSCs), and regulatory T cells (Tregs), that promote an
155 immunosuppressive microenvironment when bioinstructed by CAFs and cancer cells (Wang
156 et al., 2020). In pancreatic cancer TAMs comprise a major component of immune cell
157 populations. The synergistic crosstalk between cancer cells and CAFs (*e.g.*, via IL-10 and
158 IL-13 secretion), in turn promotes macrophage polarization towards a TAM phenotype (*i.e.*,
159 CD136⁺ and CD204⁺), that exerts tumor-promoting functions by secreting several growth
160 factors, namely IL-10 which prevent dendritic cell-mediated antitumor immune
161 responses.(Murakami et al., 2019; Wang et al., 2020) Moreover, a crucial subset of
162 pancreatic CAFs expressing MHC class II and CD74, has shown to exhibit antigen
163 presenting capacity, stimulating CD4⁺ T cells and consequently modulating the immune
164 response in pancreatic cancer.(Elyada et al., 2020) Recognizing and modulating the nature
165 of this complex and evolving tumor-stroma crosstalk is crucial for bioengineering evermore
166 physiomimetic *in vitro* PDAC models with improved in pre-clinical/clinical correlation of
167 therapeutics performance.(Sahai et al., 2020)
168

169 **3. Engineering Blueprints for Pancreatic Tumor - Stroma Models: Elements and Tools**

170 Considering the multifarious nature of pancreatic cancer TME, the identification and
171 biophysical characterization of its fundamental cellular and matrix elements, followed by
172 their re-engineering from the bottom-up can unlock the generation of highly organotypic
173 tumor-stroma *in vitro* platforms for screening candidate therapeutics targeted to malignant
174 and/or stromal components.

175 Up to date, a plethora of techniques can be leveraged for a comprehensive deconstruction
176 and characterization of native pancreatic tumor-stroma heterogeneity, hallmarks (*e.g.*, gene
177 expression patterns, activation/de-activation of signaling pathways), as well as of major
178 biomarkers (*e.g.*, specific growth factors, cytokines, etc.). Such techniques can in turn also
179 be employed for subsequent physicochemical characterization of user-programmed 3D *in*
180 *vitro* platforms, allowing researchers to evaluate models' similarity to native human tumors
181 (**Fig.1**). In this focus, methodologies based on high-content approaches such as: (i) single-
182 cell RNA sequencing (W. Lin et al., 2020), (ii) imaging mass cytometry (Chang et al., 2017),
183 (iii) multi-dimensional fluorescence imaging (Little et al., 2020), (iv)
184 metabolomics/lipidomics (Gaspar et al., 2019), (v) multiplex ELISA (Hachey and Hughes,
185 2018) and (vi) cells and ECM proteomic profiling, conjugated with advanced bioinformatics
186 analysis, have truly opened new opportunities to deepen our understanding of intricate
187 tumor-stroma interactions and to pinpoint the numerous sub-populations/phenotypes present
188 within pancreatic cancer TME.(Steele et al., 2020)
189

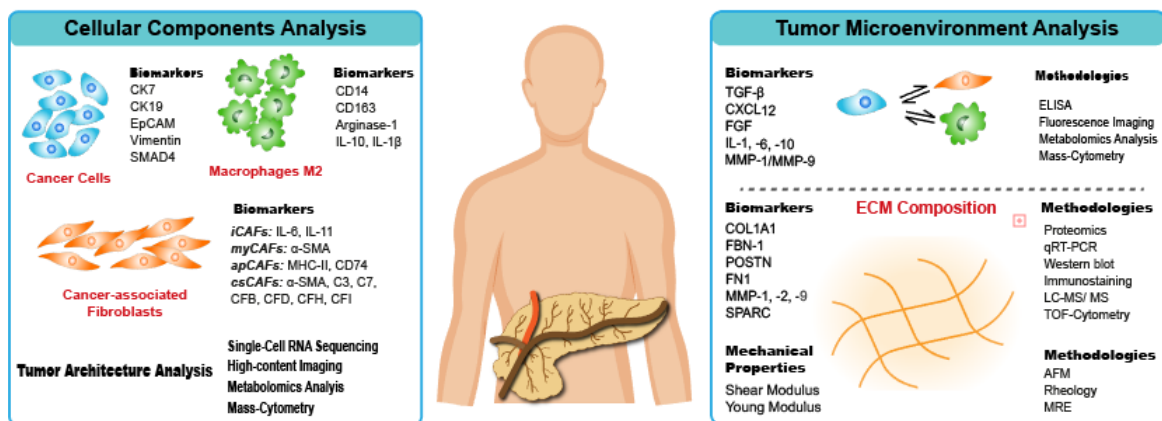


Fig.1. Schematic overview of major pancreatic cancer TME components, biomarkers, and advanced methodologies for their analysis. Characterization of key disease hallmarks during and after the bioengineering of 3D tumor-stroma platforms can open new avenues in improving their ability to emulate the *in vivo* scenario. Moreover, patients' tumor characterization a priori to the engineering of tumor-stroma *in vitro* models may unlock the potential for personalized and precision medicine approaches.

The highly relevant data libraries generated by such methodologies constitutes a unique opportunity for identifying and recapitulating the correct cellular elements and phenotypes in engineered preclinical models. This bioengineering roadmap based on the use of advanced characterization tools for supporting an informed generation of 3D *in vitro* tumors is widely transversal beyond pancreatic cancer. Indeed, this multi-dimensional strategy based on an initial TME profiling followed by rational 3D models biodesign and subsequent physiological characterization upon *in vitro* culture along time, can be viewed as a universal blueprint for engineering other malignancies in which tumor-stroma interactions are recognized to play a crucial role (*e.g.*, breast, lung, colorectal, etc.). This strategy could also be further extended toward personalized medicine approaches if one considers that patients' tumor-stroma could be profiled and then re-engineered in a laboratory setting for screening precision therapeutics.

Focusing on the early design stages specific for pancreatic tumor-stroma *in vitro* models, researchers must consider the inclusion of a wide array of elements and features including: (i) biological gradients establishment (*i.e.*, nutrients, metabolites, gas exchange), (ii) malignant and stromal phenotypes/heterogeneity, (iii) tumor-stroma cytoarchitecture, (iv) cell population ratios (*i.e.*, cancer-to-stroma ratios), as well as (v) tumor supporting ECM composition/mechanical properties. Recapitulating many of these aspects, as well as characterizing their influence in 3D pancreatic cancer model's physiology is key for bioengineering increasingly biomimetic testing platforms. All in all, introducing major stromal cells and ECM components is the key to recapitulate TME hallmarks as these are the main orchestrators of pancreatic cancer pathophysiology.

3.1. Living Stromal Elements in 3D Pancreatic Cancer Models – Bioengineering and Phenotyping

Considering that CAF stromal units are major living orchestrators of desmoplastic reaction in pancreatic cancer TME, their rational inclusion in a mode that accounts for malignant-stroma ratios is an important aspect that needs to be emulated for improving 3D tumor models correlation with the *in vivo* scenario. (Tsai et al., 2018) For introducing CAFs in microtumor models in a biomimetic way that recapitulates patient tumors occupation,

228 researchers have employed histopathological analysis of human tumor tissues.(Tanaka et al.,
229 2020) Such informed design approach has evidenced that PDAC stroma may comprise 40 to
230 80 % of the entire tumor mass. On this focus, a seminal report has recently opened new
231 avenues toward advancing histology-based tumor profiling through optimization and
232 validation of an *in situ* 3D characterization/reconstruction of pancreatic cancer tumor
233 anatomy with single cell resolution and in a patient-personalized mode.(Kiemen et al., 2020)
234 The highly relevant data extrapolated from such volumetric analysis may provide major
235 advances to researchers aiming toward recapitulate multiple tumor-stroma interactions
236 including those taking place at the cellular level or more at a macroscale in the whole tumor
237 volume. Localizing CAFs distribution in 3D is a highly desirable feature that will assist in
238 bioengineering in vitro models with a more precise tumor-stroma bioarchitecture. Controlled
239 cell deposition technologies such as 3D bioprinting, bottom-up cell-laden hydrogel
240 assemblies among other will definitely play a major role in materializing these concepts in
241 disease modeling.(Gaspar et al., 2019)

242 The growing evidences of CAFs abundance in pancreatic cancer TME has led researchers
243 to better acknowledge the importance of mimicking their biological effects. As such, various
244 researchers have endeavored to recapitulate human PDAC stroma occupancy by precisely
245 tuning CAFs:cancer cells ratios (*i.e.*, CAF-to-cancer cell density introduced in cancer
246 models), in an attempt to better mimic the *in vivo* scenario in an *in vitro* setting.(Tanaka et
247 al., 2020) This parameter is crucial for enabling researchers to manipulate the desmoplastic
248 fibrotic reaction and stroma-tumor signaling in 3D *in vitro* models (*i.e.*, via growth factors,
249 cytokines, vesicles, etc.). Tuning this ratio according to different disease stages (*i.e.*, stage
250 0 - carcinoma *in situ*, up to stage 4 – confirmed spreading to other organs), has remained
251 rather underexplored in 3D *in vitro* models and we anticipate that the combination of high-
252 content cell characterization methodologies combined with advanced bioengineering tools
253 will unlock the generation of stage-specific tumor surrogates for precision medicine
254 approaches.

255 Adding to this, during 3D models design stages CAFs heterogeneity is another key aspect
256 that must be considered, since a growing body of evidence indicates that these sub-cellular
257 populations exhibit different phenotypes, ultimately influencing tumor progression and drug
258 resistance through multiple cell-protecting mechanisms.(Pereira et al., 2019) Exploiting this
259 heterogeneity may unlock new avenues and strategies regarding the discovery of novel
260 biological targets for disrupting the pancreatic tumor-stroma interplay.

261 Generally, CAFs phenotype is characterized by an altered expression of alpha-smooth
262 muscle actin (α -SMA), fibroblast activation protein (FAP), and S100A4.(Grünwald et al.,
263 2021; Olive, 2015) CAFs can also display increased proliferative markers and motility, as
264 well as cytoskeletal re-arrangement.(Erdogan and Webb, 2017; Han et al., 2020).
265 Importantly, most activated CAFs secrete soluble growth factors and chemokines such as
266 TGF- β , platelet derived growth factor (PDGF), chemokine (C-X-C motif) ligand 2 (CXCL2)
267 and endothelin. (Schnittert et al., 2019; Zhan et al., 2017) CAF-associated secretome has
268 been routinely characterized through conventional approaches (*i.e.*, ELISA or western blot).
269 More recently, the establishment of advanced mass-spectrometry characterization
270 approaches has led to the discovery of an additional array of characteristic biomarkers
271 correlated with CAFs bioactivity having enabled the identification of multiple
272 phenotypes.(X. Liu et al., 2017; Santi et al., 2017) Gathering on these approaches, up-to-
273 date 4 main subtypes of pancreatic CAFs have been identified and classified according to
274 their biomarkers/phenotypes, namely: (i) inflammatory CAFs (iCAFs), which lack α -SMA
275 expression and exhibit high expression of inflammatory mediators (*e.g.*, IL-6, IL-11) being

276 located in the peripheral regions of the main tumor, (ii) juxtatumoral myfibroblasts
277 (myCAFs), which express high levels of α -SMA and low levels of inflammatory mediators,
278 (iii) antigen-presenting CAFs (apCAFs) that exhibit a combination of iCAF and myCAF
279 biomarkers expressing low levels of α -SMA and IL-6, but expressing MHC-II and CD74,
280 and (iv) complement-secreting CAFs (csCAFs) which express high levels of α -SMA and
281 complement associated factors (*e.g.*, C3, C7, CFB, CFD, CFH, CFI), having only been
282 recently identified.(Chen et al., 2021) Interestingly, the direct interplay of csCAFs with
283 pancreatic cancer cells has only been observed in early tumor development, leading to
284 important insights regarding their inclusion in 3D tumor models that aim to mimic different
285 disease stages.(Chen et al., 2021; Sun et al., 2018)

286 Such heterogeneity not only highlights CAFs multifactorial influence in pancreatic cancer
287 TME but also accounts for their possible role as important mediators of tumor immune
288 response.(Schnittert et al., 2019) CAF-mediated desmoplasia is in turn correlated with
289 increased pancreatic tissue stiffness that consequently induces blood vessel
290 collapse.(Chronopoulos et al., 2017; Sugimoto et al., 2014) Currently available cell
291 processing/engineering technologies such as cell sheets, hydrogel stacking, 3D bioprinting
292 and/or organoid engineering could foreseeable help further develop models capable of
293 integrating such population specific interactions in a mimetic platform.(Reid et al., 2019)

294 Metabolic profiling may also provide important insights in 3D pancreatic cancer models
295 bioengineering since aberrant metabolism is a well-established hallmark of this
296 neoplasia.(Knudsen et al., 2016) CAFs play an important role on PDAC metabolism shift as
297 they undergo a metabolic transition from oxidative phosphorylation to glycolysis (*i.e.*,
298 Warburg effect), over producing lactate, ketone bodies, glutamine, and fatty acids, which are
299 then secreted and exploited by surrounding cancer cells to sustain their
300 proliferation.(Broekgaarden et al., 2019; Sazeides and Le, 2018) Moreover, it has been
301 evident that CAFs-derived alanine used in the TCA cycle also promote tumor growth in low-
302 nutrient environments. Such, allows glucose to be used in nucleic acids synthesis, further
303 accelerating cancer cells proliferation.(Sazeides and Le, 2018) As metabolic reprogramming
304 plays a key role in carcinogenesis and therapy responsiveness, the recapitulation and study
305 of such metabolic profiles *in vitro* can be useful to develop diagnostic techniques and to
306 facilitate the identification of novel therapeutic targets.

307 Other living stromal elements such as immune system cells, particularly TAMs, are also
308 key effectors in pancreatic cancer stroma, exhibiting a major influence in tumor progression
309 and therapy resistance. These microenvironment reactive cells are generally recruited to the
310 vicinity of cancer cells with increasing evidences demonstrating that their bioactivity and
311 phenotype is closely related with M2-like polarized macrophages.(Lankadasari et al., 2019)
312 Although full consensus regarding the secretome of such cells is still yet to be obtained, it is
313 known that polarized TAMs contribute to tumor progression and drug resistance through
314 the secretion of major tumor supporting growth factors (*e.g.*, EGF, MMPs, VEGF, PDGF,
315 FGF, among others) and chemokines that stimulate tumor growth and trigger metastatic
316 events.(Daniel et al., 2019) During tumorigenesis, cancer cells recruit monocytes and
317 macrophages trough the secretion of specific factors (*e.g.*, CCL5, CXCL8, CXCL12, etc.)
318 that ultimately bioinstruct monocytes polarization toward an M2-like phenotype.
319 Interestingly, apart from cancer cell-derived signals, CAFs also secrete important factors
320 (*i.e.*, TGF- β and IL-10) that promote macrophages polarization. Translating such
321 environment to 3D *in vitro* platforms is critical, especially if the screening of
322 immunomodulating therapeutics is envisioned.

323 From a bioengineering perspective, TAMS installation in *in vitro* models can be
324 materialized through a number of different methodologies. In an simple, yet elegant
325 approach, researchers have been co-culturing cancer cells with monocytes (*e.g.*, derived
326 from cell lines or patient-derived cells), under specific conditions that promote the
327 establishment of M2-like polarized macrophages following exposure to cancer cells secreted
328 bioinstructive biomolecules.(Rebelo et al., 2018) However, such approach can be
329 challenging from a logistic perspective since monocytes are generally cultured in suspension
330 which can increase the complexity of their co-culture with cancer cells during regular culture
331 media changes. On a different approach, monocytes can be firstly differentiated into M0
332 macrophages (adherent cells) via a stimulating culture media (*i.e.*, generally supplemented
333 with phorbol 12-myristate-13-acetate (PMA)), and co-cultured with cancer cells, enabling
334 researchers to evaluate the potential of these engineered models to recapitulate the
335 immunosuppressive pancreatic TME.(Kuen et al., 2017) Ultimately, monocytes may also be
336 differentiated and polarized towards “M2”-like TAMs *in vitro* by stimulating monocyte-
337 differentiated macrophages with IL-4/IL-13.(Yang et al., 2021) Successfully established
338 immuno-active models via this methodology may be particularly useful for screening
339 therapeutics that inhibit monocytes differentiation (*e.g.*, Pexidartinib, PF-04136309, among
340 others), opening new opportunities to tackle pancreatic cancer.(Lankadasari et al., 2019;
341 Mantovani et al., 2017; Xiang et al., 2021) However, prior to being used for advancing
342 therapeutics screening researchers must evaluate the phenotype of differentiated
343 macrophages through specific methodologies that enable the clear detection of TAMS-
344 associated biomarkers (*e.g.*, IL-4, IL-10, IL-6, Arginase 1, CCL2, CD163, etc.)
345 **(Fig.1)**.(Kuen et al., 2017)
346

3.2. Tumor and Stromal ECM in 3D Pancreatic Cancer Models – Bioengineering and Characterization

Throughout life, healthy tissue ECM provides cells with specific biological cues recognized to activate downstream signaling events exhibiting a key role in cellular signaling and cell fate. In contrast to normal pancreatic tissues, tumor ECM is highly fibrotic, operating both as a cell bioinstructive component that drives tumor progression, resistance and metastasis, as well as constituting a major physical barrier to therapeutics delivery.(Tomás-Bort et al., 2020)

During disease progression pancreatic ECM experiences several alterations in its nano/micro-topography, stiffness, viscoelasticity and biochemical composition.(Feig et al., 2012; Nia et al., 2020; Winkler et al., 2020) Collagen is the most abundant ECM component in cancer, with fibrillar collagens (*i.e.*, COL1A1, COL1A2, and COL3A1) representing the major elements of pancreatic cancer ECM. Interestingly, an approximate 2.6-fold increase in these components has been reported to occur during progression from healthy to malignant pancreatic tissues.(Liot et al., 2021; Nabavizadeh et al., 2020; Tian et al., 2019) Such uprise in fibrillar collagen is generally mediated by enzyme-mediated collagen crosslinking, by the action of lysyl oxidase (LOX) and transglutaminase 2.(Rice et al., 2017) Overall, pancreatic cancer-associated desmoplasia results in a stiffer microenvironment exhibiting dense collagen fiber assemblies, as well as increased laminin and fibronectin deposition.(Akhter et al., 2020) Additional ECM components that are significantly overrepresented in pancreatic cancer include Fibrillin-1 (FBN-1), fibrinogens (FGA, FGB, and FGG), and periostin, most of them being commonly associated with increased invasive capacity and disruption of surrounding tissue basement membrane.(Tian et al., 2019)

Hyaluronan (HA) is also a critical ECM component found *in vivo*, playing a key role in increasing malignant tissues stiffness due to its abundant accumulation in tumor surrounding stroma along time.(Sato et al., 2016) Considering that stromal cells are the major effectors in *de novo* matrix deposition, it is important to emphasize that HA is more prevalent in pancreatic stroma ECM rather than in the main tumor, an important aspect that is yet to be widely emulated in predictive 3D preclinical PDAC models.(Bulle and Lim, 2020; Jiang et al., 2020) The widely reported aberrant HA buildup and dynamic degradation in pancreatic TME is closely associated with its poor prognosis, as demonstrated by mounting clinical evidence.(Kim et al., 2020; Sato et al., 2016) Hyaluronan with different biopolymer backbone sizes have also been found to distinctly influence tumor development, with significant deposition/degradation of high molecular weight HA (> 500 kDa) promoting an anti-inflammatory and anti-angiogenic response, while lower molecular weight HA(20–200 kDa), having been recognized to bioinstruct angiogenic and pro-inflammatory pathways.(Chang and Lin, 2021; Sato et al., 2016)

To recapitulate such biomolecular features, researchers have been focusing on engineering ECM-mimetic hydrogel biomaterials, especially proteinaceous biomaterials (*e.g.*, gelatin, collagen, human-based platelet lysates) and/or tumor tissue decellularized extracellular matrix (dECM)/basement membrane extracts which exhibit cell adhesive and bioinstructive cues in an endeavor to stimulate cancer and stromal cells bioactivity similarly to that posed by native tumor-stroma ECM elements.(Blanco-Fernandez et al., 2021; Ferreira et al., 2020; C. F. Monteiro et al., 2020; Pinto et al., 2017) Up-to-date these biomaterials have been mainly exploited for 3D disease models in the form of fibers, sponges, microcarriers and/or bulk hydrogels.(Ajeti et al., 2017; Antunes et al., 2019; Blanco-Fernandez et al., 2021; Brancato et al., 2017; Ricci et al., 2014) Owing to their high-water content, biophysical properties and similarity to tissues ECM, hydrogel scaffolds have been

395 the most widely explored scaffolds to engineer organotypic 3D models.(Liaw et al., 2018;
 396 Lin and Korc, 2018) Various reports focusing on recapitulating pancreatic cancer-stroma
 397 ECM have taken advantage of a wide range of biologically tunable hydrogels and
 398 biocompatible crosslinking approaches (*e.g.*, photo-induced, enzyme, supramolecular,
 399 bioorthogonal click-chemistry, etc.) which can be leveraged to better control ECM mimetic
 400 cell laden platforms, bioactivity, porosity, topography and dynamic mechanical properties
 401 (*i.e.*, viscoelasticity, stiffness) (Lin and Korc, 2018; H. Y. Liu et al., 2017; Liu et al., 2018).

402 Tumor-stroma ECM biophysical properties are known to be of high interest for *in vitro*
 403 tumor modelling owing to constant de novo matrix deposition/remodeling through time. To
 404 bioengineer ECM biomimetic tumor-stroma platforms that emulate matrix mechanics either
 405 in a ‘one-fits-all’ approach or in a more patient tumor-matched mode, researchers require
 406 highly sensitive characterization techniques and methodologies capable of providing tumor-
 407 stroma ECM mechanical characterization. Recent advances in mesoscale indentation force-
 408 displacement, harmonic motion/shear wave elastography (HME/SWE), atomic force
 409 microscopy (AFM) and magnetic resonance elastography have opened new opportunities for
 410 identifying native pancreatic cancer ECM stiffness.(Nguyen et al., 2016a; Zanutelli et al.,
 411 2020) Following a comprehensive analysis of literature reports employing these tools one
 412 can observe that pancreatic tumors mechanical features is highly heterogeneous, ranging
 413 from ~1 kPa to above 44 kPa (**Table 1**).(Nabavizadeh et al., 2020) Such heterogeneity may
 414 be correlated with two main factors, (i) the lack of correlation and standardization regarding
 415 ECM analysis tools/methodologies, and (ii) the intra-tumoral heterogeneity generally
 416 observed in tumor tissue samples.(Guimarães et al., 2020) All in all, this ultimately impacts
 417 3D tumor-stroma models engineering with researchers being uncertain which mechanical
 418 properties should be emulated.

419
 420

Table 1. Pancreatic tissues mechanical stiffness characterization.

Sample Type	Characterization Technique	Population size (N)	Young’s modulus (kPa)	Disease Class	Ref.
Murine Pancreatic Tumor	Harmonic motion elastography	30	11.3 ± 1.7	Stage I-II	(Nabavizadeh et al., 2020)
	Atomic force microscopy	52	4 ± 1.6	N.D.	(Rice et al., 2017)
	Harmonic motion elastography	N.D.	2.1 - 6.7	N.D.	(Nabavizadeh et al., 2018)
Healthy Human Pancreatic Tissue	Magnetic resonance elastography	22	1.13 - 2	N.A.	(Kolikopka et al., 2017)
	Mesoscale indentation	22	1.06 ± 0.25	N.A.	(Rubiano et

	Shear wave elastography	84	4.39 - 7.84	N.A.	al., 2018) (Yoshikawa et al., 2021)
Pancreatic Cancer Cell Lines	Atomic force microscopy	25-35	MIA PaCa-2: 1.7 ± 1.0 PANC-1: 2.4 ± 1.1 HPDE: 3.7 ± 1.2 Hs766T: 3.0 ± 2.0	N.D.	(Ngyen et al., 2016b)
	Magnetic resonance elastography	26	3.22 - 5.11	N.D.	(Shi et al., 2018)
	Magnetic resonance elastography	8	6.06 ± 0.49	N.D.	(Itoh et al., 2016)
	Harmonic motion elastography	32	15 - 44.8	Stage II-III	(Nabavizadeh et al., 2020)
Human Pancreatic Tumors	Mesoscale indentation	-	6 - 18	N.D.	(Rubiano et al., 2018)
	Mesoscale indentation	59	1.4 - 5.1	Stage II-IV	(Sugimoto et al., 2014)
	Shear wave elastography	22	3.48 - 11.55	Stage II-IV	(Yoshikawa et al., 2021)

*N.D. – non defined; N.A. – not applicable

421

422

423

424

425

426

427

428

429

430

431

432

433

434

435

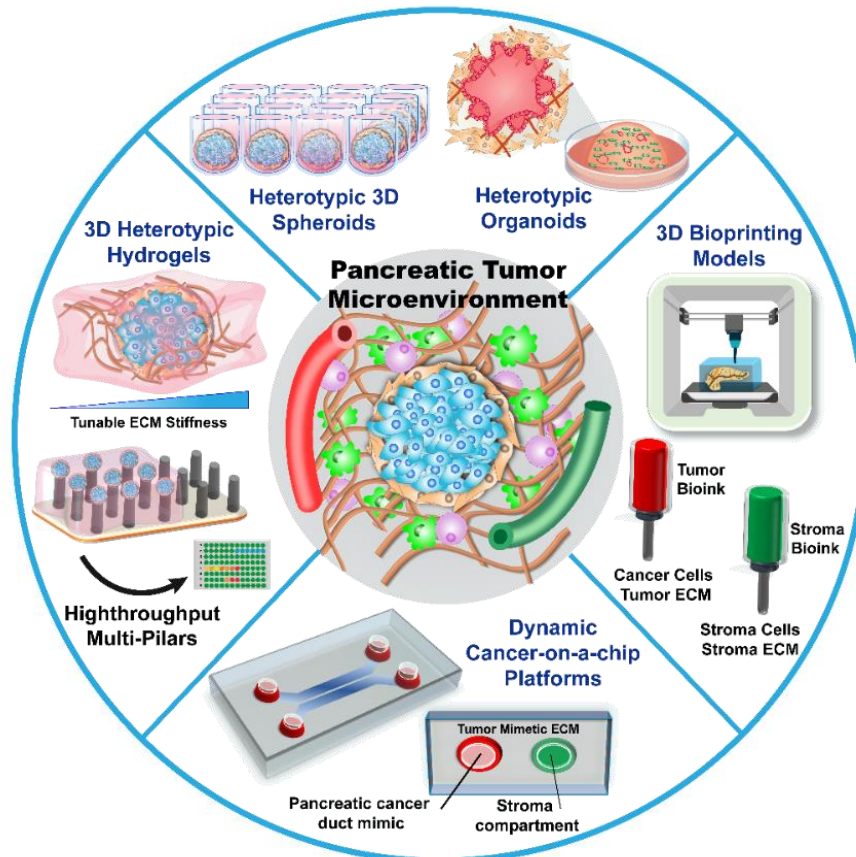
From a critical perspective, not only further improvement and standardization of mechanical characterization methods is highly required but also our understanding of the dynamic mechanical alterations that occur from early stages to later stages of tumor progression must improve to accelerate the design of increasingly organotypic *in vitro* models. On this focus, the recent exploitation of advanced liquid chromatography–tandem mass spectrometry (LC-MS/MS) characterization techniques has provided extensive portrays of pancreatic cancer ECM evolution and patient heterogeneity.(Tian et al., 2019; Weniger et al., 2018) Such big data technologies revealed an up-regulated group of matrisome proteins present in both PDAC tumor and stroma compartments and allowed researchers to associate their deposition in a cell specific manner, highlighting the importance of the stromal compartment in PDAC desmoplasia.(Tian et al., 2019) Furthermore, by defining the ECM cellular origins in LC-MS/MS these studies revealed that although the pancreatic stroma is responsible for 90 % of *de novo* ECM deposition, elevated

436 levels of ECM proteins derived exclusively from cancer cells can be directly correlated with
437 poor patient survival. Integrating these methodologies in 3D models early design stages, as
438 well as during their *in vitro* maturation may provide important information regarding
439 different models' correlation with the *in vivo* setting.

440 Holistically, the rational design of 3D pancreatic tumor-stroma models both at a cellular
441 and matrix level benefits from exploring advanced tools to characterize human tumor tissues.
442 Further down the screening pipeline, the same tools and methodologies can be leveraged to
443 follow up and characterize preclinical tumor models biomarkers and bioactivity serving as a
444 quasi-validation of 3D models' ability to recapitulate such major disease hallmarks.
445

446 **4. Advances in *In vitro* Models for Capturing Pancreatic Tumor – Stroma** 447 **Interplay**

448 Gathering on the importance of living stromal elements and supporting ECM interplay
449 with pancreatic cancer cells, researchers have been rapidly moving forward toward
450 developing more organotypic *in vitro* platforms that account for these dynamic interactions.
451 On this focus, long-term existing and rapidly emerging cell/matrix 3D culture technologies
452 (*e.g.*, cell-rich and ECM mimetic biomaterial-based platforms), alongside with big data
453 characterization tools are being actively explored as the bioengineering cornerstones for
454 materializing human disease surrogates (**Fig. 2**). Such unique synergy between fundamental
455 tumor knowledge and engineering as already let to major advances on establishing 3D *in*
456 *vitro* tumor-stroma pancreatic cancer models for preclinical validation of candidate anti-
457 cancer therapies as it will be showcased in the following sections.



458 **Fig. 2.** Overview of advanced technologies for bioengineering pancreatic tumor-stroma
459 physiommimetic *in vitro* models.
460

461

462 **4.1. Cell-rich Tumor-Stroma 3D Models**

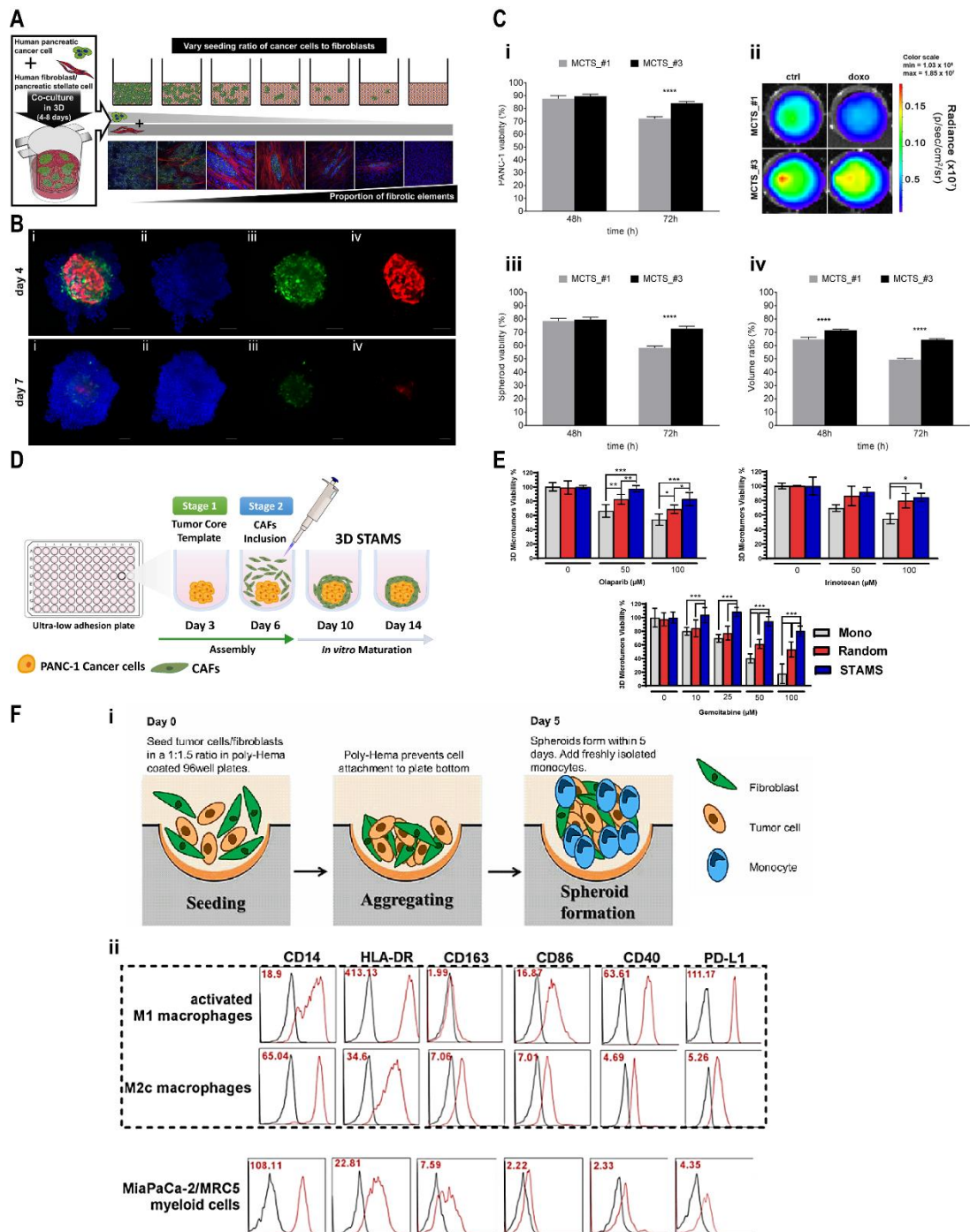
463 Spheroid models comprising randomly agglomerated cells have been among the most
464 widely explored platforms for *in vitro* tumor modelling. Spheroids highly modular nature
465 enables the introduction of multiple cell types, this combined with their easy to establish
466 unsupervised self-assembly renders them highly attractive for high-throughput screening
467 assays.(Ferreira et al., 2018; M. V. Monteiro et al., 2020b) Most importantly, 3D spheroids
468 allow researchers to reproduce key features found in *in vivo* solid tumors, including the 3D
469 architecture, the establishment of close cell-cell interactions, pH/nutrient/oxygen gradients,
470 gene and protein expression profiles, as well as activation of drug resistance
471 mechanisms.(Costa et al., 2016) Currently, various technologies are available for 3D
472 spheroids generation, including: (i) ultra-low attachment (ULA) surfaces, (iii) hanging drop
473 technique, (iii) stirring bioreactors, and (iv) magnetic levitation, among others.(Ferreira et
474 al., 2018; Tomás-Bort et al., 2020)

475 Aiming to recapitulate the stromal components of pancreatic cancer, a 3D *in vitro* cell-
476 rich model was recently established through direct co-culture of different pancreatic cancer
477 cell lines (PANC-1, AsPc-1, BxPC-3, Capan-1 and MIA PaCa-2) and PaSCs. Heterotypic
478 3D Spheroids incorporating PaSCs were more compact than their monotypic counterparts
479 and exhibited a prominent desmoplastic reaction with increased collagen deposition,
480 indicating the importance of including these stromal elements.(Ware et al., 2016)

481 Seeking to further investigate the role of fibrotic elements within pancreatic cancer TME,
482 researchers recently devised an elegant heterotypic cell-rich living platform that enables a
483 precise tuning of the ratio of fibrotic elements *in vitro*. The established 3D cell-culture
484 technique was based on the use of a culture platform (*i.e.*, transwell type inserts) to enable
485 high cell density 3D tissues generation devoid of cell supporting biomaterials facilitating the
486 visualizations and analysis of 3D microtissues and respective ECM composition. To
487 materialize the tumor models, normal human dermal fibroblasts (NHDF) and PSCs were
488 embedded in fibronectin:gelatin and combined with PDAC cells with user-programmed
489 cellular ratios. The cell suspensions were then cultured in transwell cell culture inserts coated
490 with fibronectin enabling the formation of a stroma-rich compartment. PDAC cell-lines were
491 then combined either with NHDF or human PDAC-derived PSCs at various seeding ratios
492 to cover the clinically observed range of stroma proportion in PDAC tissues. Although such
493 methodology was functional for several PDAC cells:NHDF/PSCs combinations, the
494 assembly of living 3D microtissue models is highly dependent on tumor cell-associated
495 expression of E-cadherin. Moreover, researchers were able to analyze the molecular
496 mechanisms that lead to the acquisition of a myofibroblastic phenotype by normal fibroblasts
497 when co-cultured with PDAC cells, also having demonstrated that the acquisition of such
498 phenotype is dependent of the concerted activities of SMAD2/3 and YAP in fibroblasts (**Fig.**
499 **3A**).(Tanaka et al., 2020)

500 Similarly, a tumor-stroma 3D PDAC spheroid model comprising heterotypic triple co-
501 culture of pancreatic cancer cells (PANC-1), fibroblasts and vascular endothelial cells was
502 bioengineering in non-adherent plates (**Fig. 3B**).(Lazzari et al., 2018) The triple co-culture
503 aimed to replicate the *in vivo* microenvironment, being observed that cancer cells exhibited
504 reduced sensitivity to chemotherapeutics when compared to their monotypic 3D spheroid
505 counterparts, thus more closely mimicking tumor resistance generally observed *in vivo* (**Fig.**
506 **3C**). These evidences further support the relevance of recapitulating key cancer-stromal
507 elements in preclinical models' bioengineering and validation stages.

508 Despite such 3D models recreate PDAC tumor-stroma interplay, they still fail to emulate
509 the native compartmentalized tumor architecture which is widely recognized to significantly
510 impact cancer cells response to therapeutics.(Koikawa et al., 2018; Kota et al., 2017; Pothula
511 et al., 2020) Aiming at advancing cell-rich models in this direction, 3D organotypic
512 spheroids comprising pancreatic cancer cells and CAFs at specific ratios were recently
513 generated in an endeavor to simulate the native PDAC-stroma stratified bioarchitecture and
514 desmoplastic features.(Monteiro et al., 2021a) Such models – so termed STAMS- were
515 assembled in ultra-low adhesion (ULA) plates following an easy to implement two-step
516 strategy. Firstly, pancreatic cancer cells we self-assembled into 3D spheroids and matured
517 for 6 days to establish a template tumor core. Subsequently, CAFs were administered to pre-
518 formed 3D spheroids and allowed to autonomously self-organize, ultimately establishing a
519 cell-rich semi-enclosed layer around the original tumor core (**Fig. 3D**). This *in vitro* model
520 was shown to better recapitulate the native pancreatic tumor bioarchitecture in which cancer
521 cells are enveloped by the highly fibrotic stroma. Interestingly, the *in vitro* assembled
522 STAMS exhibited key PDAC biosignatures found in human tumors including abundant
523 collagen deposition, secretion of key molecular markers (*e.g.*, TGF- β , FGF-2, IL-1 β and
524 MMP-9), as well as resistance to standard-of-care and precision therapeutics (**Fig.**
525 **3E**).(Monteiro et al., 2021a) Such spatially organized tumor-stromal models may represent
526 a valuable strategy with increased potential for drug discovery and preclinical screening of
527 breakthrough therapies targeted to the tumor-stroma axis.



528
529
530
531
532
533
534
535
536
537
538
539

Fig.3. Pancreatic cancer tumor-stroma, cell-rich 3D *in vitro* models. (A) Schematic of 3D PDAC fibrotic tissue assembling by pancreatic cancer and PaSCs co-culture at different ratios. Adapted from (Tanaka et al., 2020) with permission of Elsevier. (B) Fluorescence micrographs of 3D MCTS comprising PANC-1: MRC-5: HUVECs, at day 4 and day 7. Blue: nuclei, green: GFP-expressing MRC-5 fibroblasts and red: RFP-expressing HUVECs. (C) Heterotypic tumor-stroma triple co-culture model. (i) 3D Pancreatic cancer cells response to doxorubicin treatment (0.5 μ M). (ii) Representative bioluminescence images of control and treated monotypic (MCTS_#1) and heterotypic (MCTS_#3) spheroids. (iii) Spheroid viability after doxorubicin exposure (0.5 μ M) for 48 h and 72 h. (d) Inhibition of spheroid growth following doxorubicin treatment. Adapted from (Lazzari et al., 2018) under the Creative Commons CC-BY-NC-ND license. (D) Schematics of 3D stratified PDAC models assembly by using ultra-low adhesion plates. (E) Cell viability analysis of:

540 PANC-1 monoculture 3D spheroids (Mono); PANC-1:CAF spheroids, were cells are randomly
541 distributed (Random); and Stratified PANC-1:CAF spheroids (STAMS), following treatment with
542 Olaparib, Irinotecan or Gemcitabine, at day 14 of culture. Adapted from (Monteiro et al., 2021a)
543 with permission from Wiley-VCH. (F) (i) Schematics of 3D tri-culture PDAC model generation, and
544 (ii) Polarization of monocytes-derived macrophages into M2 phenotype after co-culture with cancer
545 cells: fibroblasts spheroids. 3D co-culture macrophages cell surface markers were compared to *in*
546 *vitro* M2 differentiated macrophages by flow cytometry. 3D co-culture macrophages exhibited
547 increased expression of CD14 and CD163, typical markers of M2 macrophages. Adapted from (Kuen
548 et al., 2017) with permission from PLOs One under the terms of the Creative Commons Attribution
549 License.

550

551 Adding to stromal fibroblasts, pancreatic cancer TME is also affected by immune cells
552 infiltration and clinical evidences indicate that the presence of pro-tumoral immune cells
553 such as regulatory T-cells, TAMs with M2-like polarization and myeloid-derived
554 suppressive cells (MDSCs) in primary tumors might be correlated with tumor
555 progression. (Karamitopoulou, 2019; Wörmann et al., 2014) Among these, TAMs have been
556 extensive associated with poor prognosis in more than 80 % of all pancreatic cancers owing
557 to immune-suppressive cytokines secretion (*e.g.*, IL-1, -6, -10 and TGF- β). (Pathria et al.,
558 2019)

559 Recently, an immunocompetent 3D heterotypic triple model comprising pancreatic
560 cancer cells, lung-derived fibroblasts and monocytes was established to emulate these tumor-
561 stroma interactions (**Fig.2F,i**). (Kuen et al., 2017) In this TME surrogate setup the dynamic
562 interplay between cancer cells and fibroblasts led to the release of immunosuppressive
563 mediators and consequently to the differentiation of 3D cultured monocytes in TAMS
564 exhibiting an M2-like phenotype, a major aspect considering that this event also occurs *in*
565 *vivo* (**Fig.2F,ii**). Following the administration of T-cells to the tri-culture immunocompetent
566 spheroid, macrophages inhibited CD4+ and CD8+ T-cell proliferation and activation. Such
567 findings are particularly relevant and advantageous to model *in vitro* if the screening of
568 candidate immunotherapeutics is envisioned. In fact, considering that pancreatic cancer is
569 one of the most challenging neoplasia's to tackle via immunotherapy due to its renowned
570 immunosuppressive environment, developing new testing platforms that recapitulate this
571 major hallmark and multi-cellular population dynamics may pave the way to accelerate the
572 discovery of bio-relevant immunotherapies.

573 Nevertheless, from a critical perspective, the groundbreaking advances in pre-clinical
574 drug screening provided by cell-rich 3D spheroid platforms are not without some limitations,
575 being one of the most important the lack of a pre-existing ECM in early culture time
576 points. (Pradhan et al., 2017) Installing, ECM-associated biomolecular cues will activate
577 mechanotransduction pathways, trigger different cellular phenotypes and introduce
578 additional mass transport limitations, all of which are critical aspects that cannot be
579 accurately replicated in standard 3D spheroids. (Pradhan et al., 2017) As such, the
580 development of more physiomimetic PDAC models that accurately mimic pancreatic cancer
581 *in vivo* TME cellular and ECM stromal components are being actively pursued.

582

583 **4.2. Biomaterial-based Pancreatic Cancer-Stroma Models**

584 Engineered biomaterial-based models comprising naturally-derived and/or synthetic
585 biomaterials aiming to function as ECM-mimetic cell-supporting scaffolds have proven to
586 be a valuable tool for recapitulating this key stromal component found in living
587 tissues. (Wang et al., 2014) Gathering on this, natural-derived biomaterials arise as a
588 particularly attractive alternative to recapitulate this component *in vitro* owing to their ECM-

589 like features (*i.e.*, viscoelasticity, high water content, tunable mechanical properties, display
590 of bioinstructive/cell adhesive motifs). Up-to-date, a wide range of ECM mimicking
591 biomaterials have been employed for modelling tumor ECM components *in vitro* including:
592 (i) gelatin, (ii) collagen, (iii) hyaluronic acid and (iv) dECM.(Lin and Korc, 2018) Aiming
593 to recapitulate *in vivo* tissues, collagen matrices have been exploited to model the migration
594 behavior and invasion profile of pancreatic cancer cells. These hydrogels were installed in a
595 custom-built high-throughput, high-content drug screening platform for providing the
596 establishment of co-cultured 3D spheroid models comprising PDAC cells and CAFs
597 surrounded by oligomeric type I collagen, (**Fig. 4A**).(Puls et al., 2018) Such high-throughput
598 platform can accelerate the screening and preclinical validation of novel drugs in an effective
599 manner when introduced in automated bioimaging systems, overcoming the laborious
600 aspects and limitations of standard platforms.

601 On a similar focus, Matrigel has also been considered as a gold-standard for 3D hydrogel-
602 based tumor modelling. Matrigel is a complex protein mixture derived from the basement
603 membrane of Engelbreth-Holm-Swarm (EHS) mouse sarcoma a highly complex
604 biomolecule mixture rich in collagen IV, laminin, heparin sulfate proteoglycans, as well as
605 a variety of growth factors (*e.g.*, TGF- β , FGF, epidermal growth factor, PDGF) that
606 constitute the original tumor TME from which this processed basement membrane is derived
607 from.(Hughes et al., 2010; Lin and Korc, 2018) Due to its biological origin, Matrigel-based
608 scaffolds have been widely exploited for engineering 3D *in vitro* PDAC models for
609 investigating cells invasion potential and anti-cancer drugs efficacy, among other
610 applications.(Lin and Korc, 2018) Despite being successful in supporting human cancer cells
611 culture, Matrigel is an animal-derived biomaterial, is highly variable from batch-to-batch
612 and its mechanical properties are challenging to be tailored to those of pancreatic cancer
613 tissues. These undesirable features render Matrigel a sub-optimal option for accurately
614 recapitulating pancreatic TME biophysical and biochemical properties.(Benton et al., 2014)

615 Hydrogel-based scaffolds generated from well-defined synthetic materials (*e.g.*, PEG,
616 PLA, PCL, etc.) have also been exploited to model the pancreatic tumor-stroma interplay *in*
617 *vitro*. Due to their poor bioactivity and low correlation with ECM components, biomimetic
618 peptides (*e.g.*, MMP cleavable peptides, RGD peptides, etc.) alongside with chemical
619 crosslinking moieties (*e.g.*, acrylate, tyrosine, etc.) are commonly conjugated with synthetic
620 polymers to imprint organotypic features to these scaffolds.(H. Y. Liu et al., 2017) However,
621 such approaches fail to fully recapitulate the intrinsic bioactivity of proteinaceous
622 biomaterials.

623 Hyaluronic acid (HA) is yet another important stromal component that must be introduced
624 during the engineering of pancreatic tumor-stroma models since it is widely recognized that
625 this glycosaminoglycan (GAG) is over-expressed and accumulated in PDAC stroma.
626 Importantly, the presence HA has been closely related with a poor patient outcome, owing
627 to its contribution for cancer cells proliferation, activation of invasion mechanisms and
628 multi-drug resistance.(Olive, 2015) Although unmodified HA does not support integrin-
629 mediated cell adhesion, it can interact molecularly and activate CD44 and RHAMM
630 (CD168) receptors in cells present in the pancreatic TME.(Sapudom et al., 2020) In addition
631 to its biological relevance, from a chemical engineering point of view HA backbone is highly
632 versatile being amenable for chemical modification through the conjugation with numerous
633 moieties (*i.e.*, norbornene, thiol, amine, boronate, etc.)(Liu et al., 2018) Most commonly, HA
634 has been chemically modified with methacrylate and thiol moieties to produce
635 photocrosslinkable hydrogels with tunable mechanical properties and biodegradation.(Liu et
636 al., 2018; Shih et al., 2016) This versatility aids on its processing into ECM mimetic

637 hydrogels and renders HA one of the most researched biopolymers for disease modelling.
638 Particularly, due to its relevance in PDAC stroma, several studies have employed HA-based
639 hydrogel scaffolds to assemble 3D *in vitro* pancreatic tumor models.(Liu et al., 2018; Wong
640 et al., 2019)

641 Recently hyaluronan grafted chitosan (CS-HA) platforms were engineered as a strategy
642 to recapitulate tumor pathophysiology, probe cancer cell-CAFs interactions and to screen for
643 anti-cancer therapeutics effectiveness. 3D heterotypic spheroids were assembled on these
644 systems by co-culturing pancreatic cancer cells and PSCs (1:9 cell-to-cell ratio).(Wong et
645 al., 2019) In essence, such HA-rich scaffolds were employed to mimic the PDAC TME
646 where the abundance of HA is an indicator for the lower prognosis.(Apte et al., 2013) The
647 established co-culture spheroids exhibited a 3D core-shell type structure and up-regulated
648 expression of stemness and migration markers, displaying potent *in vitro* tumorigenicity
649 (**Fig. 4B,C**). The developed PDAC model enabled to recapitulate the HA-enriched TME,
650 and exhibited *in vivo*-like chemoresistance, with cells also displaying a more physiomimetic
651 invasive and metastatic phenotype. Despite providing an interesting advancement, the
652 mechanics of cell-supporting ECM remained unaddressed, a particularly relevant feature if
653 one envisions to mimic the natural ECM dynamics occurring *in vivo*.

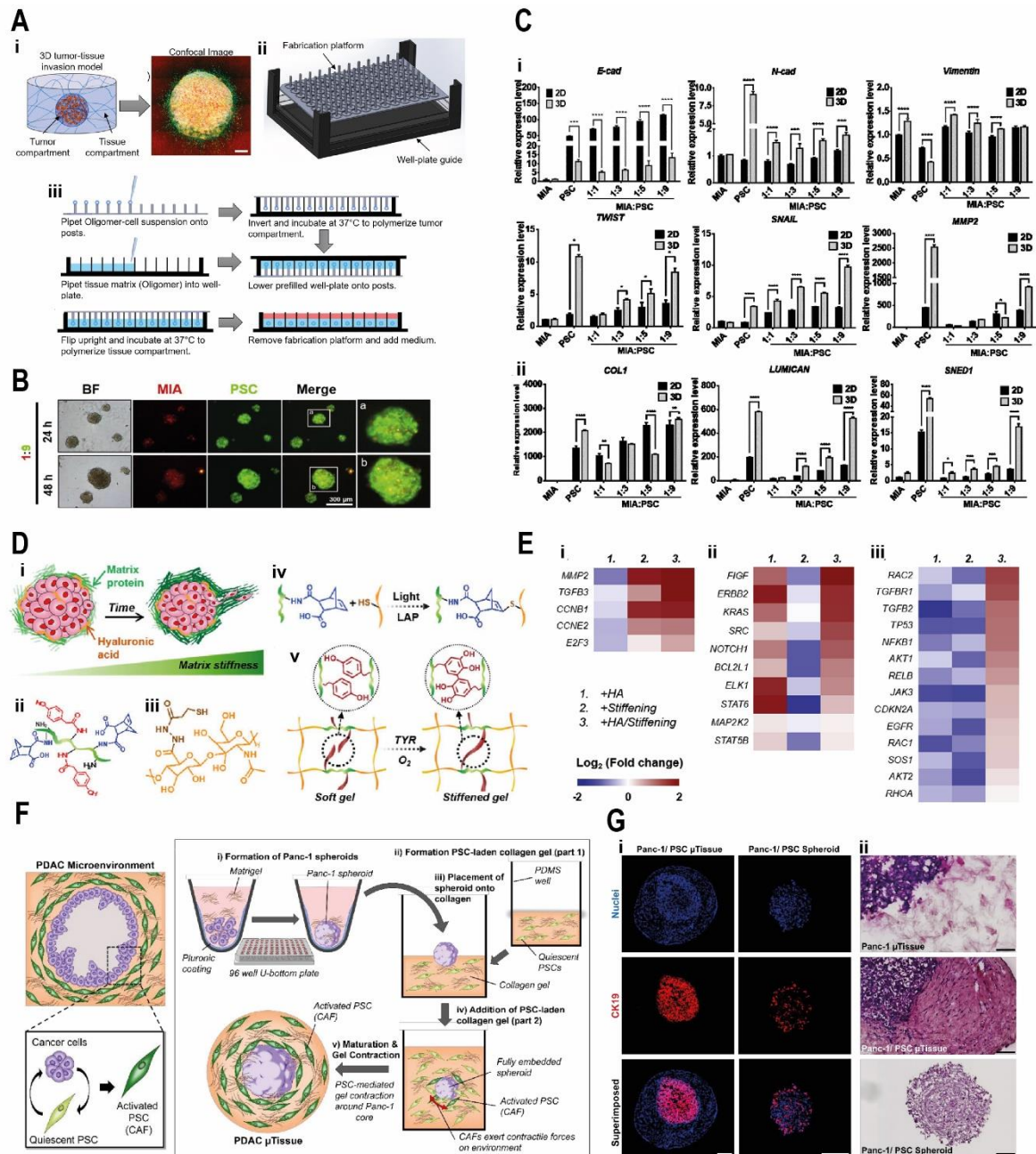
654 Aiming to replicate ECM mechanical properties and the increased stiffness of pancreatic
655 cancer TME, a mechanically tunable 3D *in vitro* system was designed by modulating
656 collagen I hydrogel stiffness to achieve PDAC-tissue specific mechanics. In this approach,
657 the viscoelastic properties of human malignant tumor, pancreatitis and healthy tissue were
658 evaluated and compared with the developed 3D *in vitro* model.(Rubiano et al., 2018) As
659 previous stated, PDAC lethality is largely correlated associated with its protective
660 desmoplastic barrier, promoting their survival and delaying the chemotherapeutics agents
661 delivery.(McCarroll et al., 2014) In addition to malignant tissue, pancreatitis is also
662 accompanied by increased stiffness, therefore, mechanical characterization of healthy,
663 pancreatitis and PDAC tissues could be an important insight to avoid misdiagnosis. In this
664 particular study, both pancreatitis (2.15 ± 0.41 kPa) and tumors (5.46 ± 3.18 kPa) exhibit
665 higher stiffness (in shear modulus) than normal tissue (1.06 ± 0.25 kPa).(Rubiano et al.,
666 2018) To mimic the PDAC remodeling behavior, stromal cells were isolated from human
667 PDAC tumors, laden in collagen hydrogels and cultured in cancer cell-conditioned medium,
668 as a strategy to prime their response to paracrine signaling and modify their
669 microenvironment. This has demonstrated the importance of tuning the mechanical
670 properties of the cell supporting matrix employed for *in vitro* maturation of the models,
671 however, a physiomimetic and dynamic stiffening of the matrix in a user programmed mode
672 was still challenging to implement in this set-up. The construction of an *in vitro* system that
673 recapitulates the *in vivo* stiffening of PDAC is an invaluable asset to probe the biomechanics
674 that underly tumor growth and metastasis, ultimately assisting in the discovery of innovative
675 therapeutics.(Rubiano et al., 2018)

676 On this focus, an elegant biomaterial-based model was developed for mimicking the
677 unique ECM stiffening dynamics and fibrotic PDAC microenvironment that are at play
678 during disease progression.(Liu et al., 2018) To recapitulate the stiffening events a double-
679 network dynamic gelatin-hyaluronic acid hybrid hydrogel with modular thiol-norbornene
680 photopolymerization (*i.e.*, U.V. light) and on-demand enzyme-triggered matrix stiffening
681 was developed. Following thiol-norbornene gelation, the tyrosine residues present in gelatin
682 macromers, were used as substrates to establish a secondary polymerization by exogenously
683 added tyrosinase, which catalyzes di-tyrosine crosslinking and increases hydrogel
684 crosslinking density and stiffness. This enables researchers to recapitulate the mechanical

685 changes suffered by TME during the desmoplastic reaction and to evaluate the influence of
686 matrix composition and dynamic stiffening on PDAC cells phenotype and bioactivity
687 (**Fig.4D**). In this hydrogel platform encapsulated cancer cells exhibited human tumor-like
688 phenotypes and increased invasiveness in stiffened gelatin-HA containing hydrogel
689 (**Fig.4E**). Despite unlocking dynamic PDAC matrix stiffening, relevant stromal cell
690 populations were yet to be included in these systems. One could hypothesize that the
691 inclusion of stromal CAFs in conjugation with on-demand stiffening could provide a fine
692 tuning of *in vitro* microenvironment mechanical properties. These approaches are envisioned
693 to increase the similarity of these models with the native tumor tissue biophysical features
694 according to tumor stage, an aspect that remains largely underexplored in disease modelling.

695 Besides the fibrotic and dense stroma, tumor-stroma hydrogel-based models have been
696 developed to resemble the unique PDAC bioarchitecture. In such work, PDAC microtissue
697 (μ tissue) models were bioengineered in order to recreate PDAC bioarchitecture as found *in*
698 *vivo*, where tumor niche is surrounded by a fibrotic stroma mainly composed by CAFs and
699 ECM components in a juxtatumoral position (**Fig.4F**). The developed tumor-stroma PDAC
700 models were assembled by seeding a pre-matured PANC-1 spheroid in a collagen-based
701 matrix populated by human PSCs, recapitulating the human PDAC stroma. By
702 immunostaining authors confirmed the successful envelopment of PANC-1 spheroid by
703 the PSCs-laden collagen hydrogel as CK19⁺ cells are only present in the core of the μ tissue
704 model, surrounded by the stroma-biomimetic compartment, recapitulating the native
705 scenario (**Fig.4G**). Additionally, heterotypic μ tissues exhibited significantly higher
706 expression of key tumor markers including POSTN, FN1, COL1, IL-6 and VIM highlighting
707 the biomimetic potential of the developed platform for understanding tumor-stroma
708 interactions and high-throughput assays.

709



710
 711 **Fig. 4.** Engineered biomaterial-based pancreatic cancer *in vitro* models. (A) 3D co-culture
 712 tumor like tissue-invasion model. (i) Schematic of 3D tumor-stroma invasion set-up, (ii)
 713 CAD construct of custom-designed platform gel for generating the tumor compartment, (iii)
 714 Step-wise methodology for establishing pancreatic tumor-stroma *in vitro* models. Adapted
 715 from (Puls et al., 2018) with permission of Springer Nature. (B) The morphology and
 716 viability of 3D spheroids comprising pancreatic cancer cells (MIA cells) and PaSCs seeded
 717 in a ratio 1:9 in Chitosan-Hyaluronan (CS-HA) platforms, for 24 or 48 h. (C) Gene
 718 expression profiling of 2D and 3D models cultured in CS-HA platforms. Adapted from
 719 (Wong et al., 2019) with permission from Elsevier. (D) Overview of dual crosslinked ECM-
 720 mimetic platforms. (i) Schematic of a fibrotic tumor microenvironment comprising matrix
 721 proteins and glycosaminoglycans, (ii) Norbornene (blue moiety) and hydroxyphenylacetic
 722 acid (HPA) (red moiety) functionalized gelatin, (iii) Thiol functionalized hyaluronic acid
 723 backbone. (iv and v) Schematics of thiol-norbornene U.V. light-mediated photocrosslinking

724 and on-demand tyrosinase-triggered di-HPA crosslinking. (E) Up-regulated genes in PDAC
725 cells laden hydrogel. (ii) Gelatin-Norbornene-HPA hydrogel devoid of HA, (ii) Gelatin-
726 Norbornene-HPA/HA hydrogel, and (iii) On-demand stiffened Gelatin-Norbornene-
727 HPA/HA hydrogel. Adapted from (Liu et al., 2018) with permission from Elsevier. (F)
728 Schematics of 3D PDAC tissues generation and the inherent cellular organization. (G)
729 Evaluation of PDAC tissues cellular arrangement by (i) immunofluorescence, and (ii)
730 hematoxylin-eosin staining. Adapted from [125] under the Creative Commons Attribution
731 (CC BY) license.

732

733 **4.2.1. Pancreatic Cancer-Stroma Organoid-in-Biomaterial Models**

734 3D tumor organoids, are rapidly emerging as valuable preclinical screening platforms
735 owing to their unique ability to reproduce key cellular features found in solid tumors *in*
736 *vivo*.(Granat et al., 2019) Unlike their spheroid counterparts, tumor organoids self-organize
737 into 3D architectures in a fully autonomous, cell-driven mode without requiring forced
738 adhesion to generate 3D living architectures. Most importantly, tumor organoids often
739 display tumor-specific cellular heterogeneity, gene and protein expression patterns,
740 histomorphological features and a high degree of *in vitro/in vivo* correlation in preclinical
741 drug screening set-ups.(Drost and Clevers, 2018) Particularly, patient-derived organoids
742 (PDOs) provide an unprecedented level of predictiveness and constitute a truly correlative *in*
743 *vitro* platform that can assist clinical decision making. PDOs are thus recognized as the next-
744 generation of microtumor surrogates owing to their potential for modelling original tumors
745 pathophysiological hallmarks (*e.g.*, driver mutations, resistance mechanisms activation,
746 genetic drift, etc.), as well as their cellular heterogeneity and cytoarchitecture. These living
747 microtissues can be readily established from surgically resected human tumors enabling the
748 establishment of organoids from different disease stages and with different genetic traits,
749 opening new avenues toward patient-personalized and precision medicine approaches.

750 Pancreatic tumor organoids are specifically characterized by nuclear irregularity and
751 nucleolar prominence.(M. Lin et al., 2020) Moreover, when cultured *in vitro* pancreatic
752 tumor organoids also retain gene/protein expression profiles and cellular 3D self-assembly
753 features over several passages.(Fiorini et al., 2020; Nagle et al., 2018) Conventionally, tumor
754 organoids are generated by encapsulation in ECM-mimetic biomaterials of animal-origin
755 (*i.e.*, Matrigel or collagen I). Apart from these supporting hydrogels, the successful
756 generation of pancreatic organoids requires the culture of their precursor cells under
757 precisely controlled conditions and well-defined culture media supplemented with growth
758 factors (*e.g.*, EGF, FGF), morphogens (*e.g.*, WNT modulators, Noggin), inhibitors (*e.g.*, the
759 TGF β inhibitor A8301), and supplements (*e.g.*, B27, Nicotinamide, N-Acetyl Cysteine).

760 Gathering on their remarkable potential but also recognizing their inherent limitations,
761 researchers have been pursuing the establishment of patient-derived pancreatic organoids to
762 shed further insights into tumor-stroma crosstalk, biology, progression and metastasis, as
763 well as for screening candidate therapeutics targeted at these axis.(Fiorini et al., 2020)
764 Recently, a biobank of patient derived tumor organoids, CAFs, and peripheral blood
765 lymphocytes was established to function as the starting ground for engineering more
766 organotypic models.(Tsai et al., 2018) Leveraging the isolated cells, heterotypic PDAC
767 organoids co-cultured with stromal and immune cells were successfully established in ECM-
768 mimetic hydrogels. For generating monotypic organoids, primary tumor tissues were
769 subjected to enzymatic digestion, embedded inside Matrigel domes and matured *in vitro*. For
770 heterotypic models, patient-matched CAFs alongside with organoid precursor cells were
771 laden in Matrigel domes and incubated with CD3⁺ T-lymphocytes. This highly

772 physiomimetic platform was able to recapitulate the biological barriers that impair T-cells
773 migration to the juxta-tumoral stroma compartment, ultimately protecting cancer cells. The
774 established PDAC organoids also expressed key pancreatic cancer biomarkers, such as CK7,
775 CK19 and P53. The developed organoid-based model offers a unique platform to investigate
776 innovative strategies aiming to improve lymphocyte infiltration into PDAC tissues. Despite
777 providing considerable advances with CAFs installation into tumor organoids, the stromal
778 cellular component is another major aspect that must be considered when aiming to
779 engineering increasingly physiomimetic models. In fact, growing evidences indicate that
780 different CAFs spatial organization in the TME originate multifarious sub-populations with
781 specific phenotypes and roles in tumor progression/drug resistance.

782 Aiming to emulate such diverseness, PDAC organoids were recently combined with patient-
783 derived CAFs isolated from different TME regions.(Grünwald et al., 2021) Initially,
784 researchers extensively characterized two co-occurrent stroma states - reactive and deserted
785 - with distinct spatial organization, as well as tumor promoting and chemoprotective roles
786 through multi-omics analysis. While the reactive stroma is vascularized, exhibits immune
787 infiltrates, promotes tumor progression and is more sensitive to chemotherapy. Conversely,
788 the deserted TME supports tumor differentiation and is more chemoprotective. This seminal
789 analysis generated important insights on PDAC organoids increased proliferation when
790 exposed to reactive-type CAFs conditioned media, highlighting their tumor-supporting role.
791 Having successfully established such living microenvironments, this approach was also
792 leveraged to model the effect of TME stage in organoids chemoresistance. Interestingly,
793 upon stimulating PDAC organoids with deserted-type CAF conditioned media, a higher
794 resistance to the standard-of-care Gemcitabine was observed, in comparison to organoids
795 cultured in reactive-type CAFs media. These important findings are suggestive that deserted-
796 type stroma is closely associated with resistance to therapeutics. Overall, this study showed
797 that PDAC spatially organized and heterogeneous stroma has distinct roles in promoting
798 tumor growth and response to therapeutics. Focusing on the latter, patient-derived PDAC-
799 derived organoids have been extensively employed for screening precision therapeutics (*e.g.*,
800 gemcitabine, nab-paclitaxel, irinotecan, 5- fluorouracil, and oxaliplatin), and the generated
801 data was then correlated to patients' responses. A high degree of correlation and predictive
802 potential concerning PDAC organoids enabled an informed therapeutics selection.(Huang et
803 al., 2015)

804 Owing to their organotypic features, tumor organoid-stroma models have also been
805 exploited for screening invasion/metastasis processes *in vitro*. To investigate the molecular
806 mechanisms of PDAC invasion process, human-derived PDAC organoid models were
807 established in collagen gels.(Huang et al., 2020) During the invasion assay PDAC organoids
808 exhibited two distinct patterns of invasion, one in which single cells with mesenchymal and
809 amoeboid morphology invaded the surrounding collagen matrix and another one in which
810 cells invaded collagen matrix as cohesive multicellular units. The authors found that invasive
811 phenotype is correlated with clinical features, giving the human samples rise to organoids
812 with predominantly mesenchymal invasion displaying significantly increased risk of death.
813 Moreover, they demonstrated that SMAD4 *in situ* inactivation promoted collective invasion
814 stimulated by TGF- β via non-canonical signaling, while organoids with wild-type SMAD4
815 mutation invade with mesenchymal phenotype. Overall, these organoid models can be
816 promising for studying the mechanisms underlying the PDAC invasion and investigating
817 possible strategies to inhibit PDAC invasion.

818 Tumor organoids have been commonly cultured in animal-derived matrices, most
819 prominently, Matrigel or collagen matrices. Although such hydrogels have demonstrated be

820 suitable for support organoids growth, they suffer from batch-to-batch variations and fails
821 to/ are devoid of emulate native tumor ECM mechanical properties, limiting the
822 recapitulation of native cell-ECM interactions. To surpass such issue, tumor-stroma PDAC
823 organoids have been established in synthetic hydrogels (e.g., polyethylene glycol (PEG))
824 owing to the easily mechanical tunability and modification with cell-adhesion cues enabling
825 to resemble human tumor tissue stiffness and cell-ECM interactions. In this work, a custom-
826 designed eight-arm PEG hydrogel chemically modified with adhesion-mimetic peptides
827 (i.e., fibronectin-mimetic peptide PHSRN-K-RGD, collagen– mimetic GFOGER peptide,
828 and a basement membrane-binding peptide) was synthesized to emulate cells secreted
829 proteins. The results demonstrated that PDAC organoids established relevant cell–ECM
830 interactions in PEG hydrogels allowing a similar growth kinetics and the establishment of a
831 cellular architecture and polarity similar to Matrigel cultures.(Below et al., 2021)
832 Interestingly by tuning PEG hydrogel physical properties to achieve a increasing stiffness
833 similar to the native tumor, PDAC organoids engage signaling consistent with mechano-
834 sensing showing increased nuclear translocation of YAP1 and increased Ctgf levels in
835 stiffened hydrogels. Moreover, PDAC organoids co-cultured with fibroblasts and
836 macrophages in PEG hydrogel exhibited a relevant tumor-stroma interactions, an invasive
837 and migratory behavior, demonstrating that such synthetic platform successfully support
838 tumor-stroma PDAC organoids culture.(Below et al., 2021) Overall, the established tumor-
839 stroma platform in PEG hydrogel demonstrated to support heterotypic PDAC organoids
840 growth and recapitulate key tumor hallmarks including the tumor morphology, native ECM
841 mechanical traits, the dynamic crosstalk between cancer-stroma components and invasive
842 behavior.

843 Ongoing human clinical trials exploring patient-derived organoids for drug screening and
844 metastasis are currently underway (NCT03544255, NCT03500068). Regardless of their
845 accuracy to model pancreatic malignancies and better predict clinical response, organoids
846 are still limited in their ability to represent angiogenesis and metastasis to secondary organs.
847 Therefore, combining tumor-stroma organoids with advanced bioengineering strategies that
848 enable precise cell spatial positioning, inclusion in tumor-mimetic ECM and culture under
849 physiological flow conditions are rapidly emerging as a fresh take to further improve our
850 understanding of PDAC microenvironment and improve drug discovery/screening.

851

852 **4.2.2. Modelling Pancreatic Tumor-Stroma Interplay – Emulating Form and Scale** 853 **Through 3D-bioprinting**

854 Recapitulating the complex morphology, spatial cellular arrangements and anatomic scale
855 of human tumors microenvironment is highly desired in *in vitro* disease modelling. On this
856 focus, rapidly emerging advances in additive manufacturing technologies such as 3D-
857 bioprinting are enabling a precise and sequential build-up of tissue-like constructs with well-
858 defined, user-programmed, geometries and chemical/biological gradients, among many
859 other features that are unattainable with common manufacturing technologies (i.e., micro-
860 molding, surface patterning, solvent evaporation, etc.)(Datta et al., 2018) In this approach,
861 computer aided design (CAD) encoded models are generally exploited for fabricating 3D
862 tissue-specific living architectures comprising a cell-laden ECM-mimetic biomaterial (i.e.,
863 so termed bioink), while allowing an accurate control over constructs physicochemical
864 properties and cellular distribution, on the fly during printing.(Yin et al., 2018) Considering
865 these advantages 3D-Bioprinting arises a valuable technology for rapidly generating
866 biomimetic tumor constructs, with functional complexity, tailored biological components,
867 reproducible geometry and programmable/time-adaptable mechanical properties, resembling

868 those of *in vivo* malignant tissues.(Pereira and Bártolo, 2015) The capacity to distribute
869 different cell types and ECM components in a biologically relevant 3D spatial arrangement
870 at an anatomic scale, indeed opens a myriad of possibilities form improving tumor-stromal
871 surrogates physiomimetic potential.

872 Up-to-date, *in vitro* tumor models of numerous types of malignancies including:
873 glioblastoma, breast cancer, prostate cancer and pancreatic cancer have been materialized
874 through 3D-Bioprinting technologies.(Duchamp et al., 2019; Hakobyan et al., 2020; Ma et
875 al., 2018) Aiming to replicate pancreatic cancer early development stages, high-throughput
876 spheroid arrays were recently generated by using 3D laser-assisted bioprinting
877 (LAB).(Hakobyan et al., 2020) LAB enabled the generation of different 3D microdroplets
878 comprising acinar and ductal cells and subsequent deposition in ECM-mimetic GelMA
879 receiving substrates. The fabricated models were able to mimic the earlier events in PDAC,
880 including EGFR translocation to the cell membrane and acinar-to-ductal transformation,
881 representing an excellent platform for accessing key factors that contribute to disease
882 progression.

883 In a different approach, 3D-bioprinting technology was also leveraged for investigating
884 tumor-stroma cells interaction and recapitulate the native tumor architecture. For this
885 purpose, a 3D-bioprinted heterotypic PDAC model comprising patient-derived cancer cells,
886 HUVECs and PaSCs, was successfully established.(Langer et al., 2019) In the fabricated 3D
887 constructs cancer cells were surrounded by stromal components leading to the establishment
888 of autocrine and paracrine signaling. All in all, such heterotypic microtissues exhibited
889 biomimetic tumor architectures and cellular distribution, as well as increased resistance to
890 standard of care pancreatic cancer therapeutics as researchers observed a dose-dependent
891 response of cancer cell death to treatment.(Langer et al., 2019)

892 Emulating bio-architecture, scale and physiology in 3D-bioprinted *in vitro* models of
893 pancreatic cancer is an exciting advance that is envisioned to give rise to a new generation
894 of models encoding anatomic-like scale in their design. Nevertheless, despite the fabricated
895 model recapitulates more features of human tumor-stroma interplay when compared to other
896 strategies, 3D-Bioprinting potential for recapitulating all the hallmarks of pancreatic cancer
897 is still to be fully unraveled. Particularly, the formulation of tumor ECM mimetic bioinks
898 that recapitulate major ECM components, the inclusion of key glycosaminoglycans such as
899 hyaluronan (HA) and the installation of on-demand/programmable stiffening dynamics
900 during long term maturation remain to be thoroughly explored in macro-scale tumor-stroma
901 biomimicking platforms.

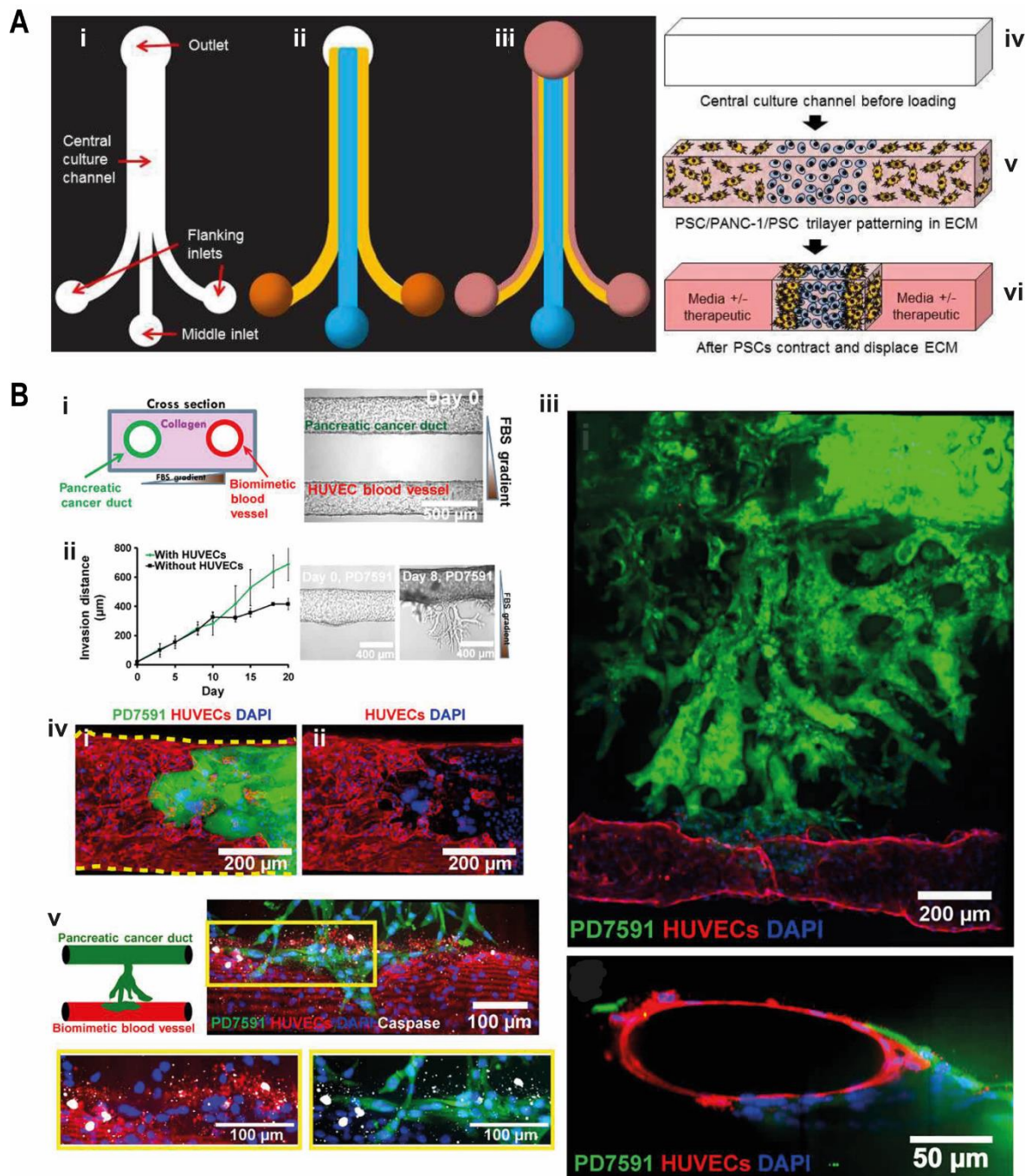
902

903 **4.2.3. Modelling Pancreatic Tumor-Stroma Interplay On-a-chip**

904 Organ-on-a-chip technologies have recently unlocked the opportunity for introducing
905 nutrient feed dynamics coupled to physiological fluid flow, shear
906 stress/mechanotransduction modulation events, and cellular/physical barriers in
907 bioengineered *in vitro* models, enabling to recreate natural features occurring in *in vivo*
908 tumors. Owing to their modular features and compatibility with optical/fluorescence
909 microscopy, microfluidic systems can also be readily adaptable for high-throughput
910 screening/high-content imaging/analytes sensing *in situ* (*i.e.*, sensing lab-on-a-chip
911 systems), enabling real-time readouts and live-imaging follow-up of 3D tumor-stroma
912 models maturation or response to therapeutics.(Carvalho et al., 2015; Shang et al., 2019)
913 Such unique features render these platforms highly attractive for bioengineering pancreatic
914 tumor-stroma heterotypic models and to probe their interplay under interchangeable/user-
915 programmed dynamic conditions that are easily controllable and reproduced *in vitro*.

916 Pioneering achievements in this direction have been recently reported via the engineering
917 of a tumor-stroma-on-a-chip for exploiting the role of tumor-stroma cell-ECM interactions
918 in a spatially-controlled 3D architecture that closely mimics the *in vivo* TME.(Drifka et al.,
919 2013) Such system was engineering by employing a microfluidic device with three inlet
920 channels that converge to form a single culture channel (**Fig. 5A**). The cell-laden ECM-
921 mimetic biomaterial was introduced through inlet ports to originate cell-rich ECM hydrogel
922 tri-layer patterns (a central cancer cell-rich layer, two flanking stromal cell-rich layers) over
923 the length of the central channel, allowing the compartmentalization of different cell types
924 without requiring artificially pre-programmed physical barriers. Aiming to accurately
925 recapitulate the heterogenous TME, a supporting ECM-mimetic dual-component hydrogel
926 (*i.e.*, collagen type I collagen/HA) was combined with human pancreatic ductal
927 adenocarcinoma PANC-1 cells and PaSCs, with the latter operating as a representative
928 stromal component due to their important role in PDAC malignancy. Collagen organization
929 was modulated via the manipulation of key polymerization parameters (*i.e.*, pH, temperature,
930 salt concentration, flow rate) to study tumor-stroma interplay and cell-cell interaction
931 migration under precise conditions. This compartmentalized design additionally enabled to
932 probe the performance of candidate therapeutics in a relevant TME-like context, and most
933 importantly to investigate the biophysical effects of innovative therapeutics in ECM
934 compactness and collagen re-organization following treatment with different doses.
935 Developing platforms for assessing biophysical effects in ECM stromal components is a
936 highly desirable feature, especially considering the emerging evidences that targeting these
937 biological barriers in pancreatic tumor could provide a therapeutic benefit. In a similar
938 approach and aiming to better understand and resemble such tumor-stroma paradigm, a 3D
939 vascularized PDAC model was established by co-culturing human PDAC organoids,
940 fibroblasts, and endothelial cells in a perfusable platform suited in a 96 well plate.(Lai et al.,
941 2020) The combination of patient-derived tumor organoids with organ-on-a-chip technology
942 offers a remarkable advance on the 3D modelling field, allowing to include key tumor
943 building blocks, namely tumor, stroma, and vasculature compartments, in a very integrative
944 way recapitulating not only the native tumor architectural and cellular features offered by
945 organoids but also the perfusable vasculature network, the fluid flow sensed by cells and
946 drug delivery mechanisms of native environment. Furthermore, the inclusion of a perfusable
947 vasculature enabled to recreate the drug diffusion mechanisms through the endothelium and
948 tumor ECM until reach the tumor mass, suggesting the potential of such platform to study
949 drug diffusion mechanism and evaluate anti-cancer drugs performance. The co-culture of
950 PDAC organoids with activated myofibroblasts promoted tumor organoid growth and
951 exhibited a high degree of ECM deposition followed by increased tissue stiffness suggesting
952 the key role of cancer cells- myofibroblasts crosstalk in tumor growth/proliferation and ECM
953 remodeling (Figure4BC). Particularly, heterotypic demonstrated higher deposition of ECM
954 proteins such as collagen and pro-tumoral cytokines than monotypic counterparts,
955 highlighting the biomimetic potential of the engineered model to recapitulate key pancreatic
956 tumor hallmarks. To elucidate the contribution of stromal fibroblasts into tumor organoids
957 resistance mechanisms, the heterotypic microtissues exhibited higher cellular viability after
958 gemcitabine exposure than their monotypic counterparts. Such results should be correlated
959 with the abundant collagen deposition and fibrotic matrix generated in such system. Overall,
960 the designed platform enabled to recapitulate important tumor hallmarks and opened new
961 avenues regarding to the co-culture of PDAC organoids with other stromal components and
962 their integration in a high-throughput dynamic/perfusable system.

963 Adding to therapeutics screening, tumor-on-a-chip platforms also offer the possibility to
964 investigate other complex biological hallmarks of pancreatic cancer, particularly its
965 hypovascularity. Aiming to better emulate such pancreatic cancer-vasculature interactions,
966 a rationally designed dual-channel microfluidic was recently developed.(Nguyen et al.,
967 2019) The designed tumor-vasculature-on-a-chip platform was configured into two parallel
968 hollow cylindrical channels embedded within a ECM-mimetic collagen-based 3D matrix.
969 Microfluidic channels were laden with pancreatic cancer cells and HUVECs respectively,
970 establishing the tumor and vascular compartments (**Fig. 5B**). During dynamic culture it was
971 observed that PDAC cancer cells invaded into the matrix toward the endothelial lumen and
972 removed endothelial cells originating b tumor-lined and tumor filled luminal structures, a
973 phenomenon described as endothelial ablation. These remarkable observations were also
974 validated in *in vivo* PDAC models, being verified that in both approaches PDAC invades
975 blood vessels and ablates the endothelium. In addition, this platform enabled to validate that
976 TGF- β receptor signaling reduces the ablation of endothelial cells by pancreatic cancer
977 cells.(Nguyen et al., 2019). In fact, leveraging on this platform PDAC-driven endothelial
978 ablation via activin-ALK7 pathway (TGF- β family receptors), was demonstrated to be a
979 potential key mechanism underlying PDAC poor vascularization. These are major
980 discoveries, considering that tumor re-vascularization strategies are evermore recognized as
981 potential therapeutic targets.
982



983
 984 **Fig. 5** Advanced organ-on-chip platforms to modulate pancreatic tumor-stroma interplay at
 985 a preclinical level. (A) Design and operation of the microfluidic device. (i - vi)
 986 Representation of the tri-layer patterning scheme and maturation following incubation with
 987 cultured media (pink color). Adapted from (Drifka et al., 2013) with permission from The
 988 Royal Society of Chemistry. (B) Tumor-on-a-chip organotypic model to study cancer cells
 989 vascular invasion. The microfluidic device comprises two hollow cylindrical channels that
 990 aims to recapitulate pancreatic duct and blood vessel structures embedded within a collagen
 991 matrix. Blood channel compartment was seeded with endothelial cells to form a biomimetic
 992 blood vessel. The pancreatic duct mimic was seeded with cancer cells. Adapted from
 993 (Nguyen et al., 2019) with permission from American Association for the Advancement of
 994 Science.

995

996 **5. Concluding Remarks and Future Perspectives**

997 The desmoplastic tumor microenvironment of pancreatic cancer and its unique stromal
998 compartment renders it one of the most challenging to replicate in a preclinical setting.
999 Gathering on the urgent necessity to develop increasingly physiomimetic models for both
1000 fundamental tumor biology studies and for innovative therapeutics screening, herein we
1001 showcased and discussed the most recent advances in bioengineering physiomimetic 3D *in*
1002 *vitro* platforms that recapitulate the unique tumor-stroma interplay naturally occurring in
1003 pancreatic cancer.

1004 All in all, while traditional 3D spheroid models and bulk hydrogel-based platforms are
1005 valuable for emulating key tumor-stroma interactions, generally they still fail on
1006 recapitulating 3D tumor bioarchitecture and evolution under flow. Such hallmarks can be
1007 matched by the synergistic combination of 3D biofabrication technologies with rationally
1008 designed tumor-on-a-chip devices, an emerging trend that is expected to yield important
1009 advances in the future. Moreover, the combination with patient-specific tumor organoids
1010 that exhibit organ-like self-organization and patient-matched pathophysiology have potential
1011 for giving rise to highly personalized therapeutic regimens.

1012 Although significant advances are envisioned with these platforms, and despite they
1013 already offer a great contribution for understanding tumor biology as well as to clinical
1014 decision making, the underlying complexity of the stromal compartment of this tumor still
1015 needs to be further addressed and more precisely emulated. Particularly, it will be valuable
1016 in the future to evaluate therapeutic responses in anatomic-sized heterotypic models
1017 comprising representative CAFs sub-populations and the various immune system stromal
1018 cells. Improvements in these aspects can shed light on several unanswered questions
1019 regarding cancer survival and metastasis mechanisms. Materializing this heterogeneity in
1020 cell-supporting matrices that better mimic the composition, architecture, biomolecular
1021 components, and mechanics of native ECM is also anticipated to boost the predictiveness of
1022 the new generation of pancreatic cancer preclinical models. Holistically, incorporating
1023 multiple engineering approaches to generate highly advanced tumor-stroma models and
1024 combining them with big data analytical tools (*e.g.*, omics-based analysis) prior and
1025 following *in vitro* design could be the key for recapitulating major biological hallmarks,
1026 biomarker signatures and resistance mechanisms. Importantly, these fundamental design
1027 blueprints and accumulating knowledge are not limited to pancreatic cancer being in fact
1028 widely applicable to a number of different neoplasias where a stroma-rich compartment is
1029 recognized to play a major role in disease progression (*i.e.*, breast and prostate cancers). The
1030 broader applicability of such bioengineering approaches further supports a more active
1031 development of tumor-stroma physiomimetic *in vitro* models in the foreseeable future.

1032

1033 **Acknowledgements**

1034 This work was developed within the scope of the project CICECO-Aveiro Institute of
1035 Materials, UIDB/50011/2020 & UIDP/50011/2020, financed by national funds through the
1036 Portuguese Foundation for Science and Technology/MCTES. This work was also supported
1037 by the Programa Operacional Competitividade e Internacionalização (POCI), in the
1038 component FEDER, and by national funds (OE) through FCT/MCTES, in the scope of the
1039 project PANGEIA (PTDC/BTM-SAL/30503/2017). The authors acknowledge the financial
1040 support by the Portuguese Foundation for Science and Technology (FCT) through a Doctoral
1041 Grant (DFA/BD/7692/2020, M.V.M.) and through a Junior Researcher contract
1042 (CEEC/1048/2019, V.M.G.)

1043

1044 **References**

- 1045 Ajeti, V., Lara-Santiago, J., Alkmin, S., Campagnola, P.J., 2017. Ovarian and Breast Cancer
1046 Migration Dynamics on Laminin and Fibronectin Bi-directional Gradient Fibers
1047 Fabricated via Multiphoton Excited Photochemistry. *Cell. Mol. Bioeng.* 10, 295–311.
1048 <https://doi.org/10.1007/s12195-017-0492-9>
- 1049 Akhter, F., Bascos, G.N.W., Canelas, M., Griffin, B., Hood, R.L., 2020. Mechanical
1050 characterization of a fiberoptic microneedle device for controlled delivery of fluids and
1051 photothermal excitation. *J. Mech. Behav. Biomed. Mater.* 112.
1052 <https://doi.org/10.1016/j.jmbbm.2020.104042>
- 1053 Antunes, J., Gaspar, V.M., Ferreira, L., Monteiro, M., Henrique, R., Jerónimo, C., Mano,
1054 J.F., 2019. In-air production of 3D co-culture tumor spheroid hydrogels for expedited
1055 drug screening. *Acta Biomater.* 94, 392–409.
1056 <https://doi.org/10.1016/j.actbio.2019.06.012>
- 1057 Apte, M. V., Wilson, J.S., Lugea, A., Pandol, S.J., 2013. A starring role for stellate cells in
1058 the pancreatic cancer microenvironment. *Gastroenterology* 144, 1210–1219.
1059 <https://doi.org/10.1053/j.gastro.2012.11.037>
- 1060 Baker, L.A., Tiriach, H., Clevers, H., Tuveson, D.A., 2016. Modeling pancreatic cancer with
1061 organoids. *Trends in cancer* 2, 176–190.
- 1062 Below, C.R., Kelly, J., Brown, A., Humphries, J.D., Hutton, C., Xu, J., Lee, B.Y., Cintas,
1063 C., Zhang, X., Hernandez-Gordillo, V., Stockdale, L., Goldsworthy, M.A., Geraghty,
1064 J., Foster, L., O'Reilly, D.A., Schedding, B., Askari, J., Burns, J., Hodson, N., Smith,
1065 D.L., Lally, C., Ashton, G., Knight, D., Mironov, A., Banyard, A., Eble, J.A., Morton,
1066 J.P., Humphries, M.J., Griffith, L.G., Jørgensen, C., 2021. A microenvironment-
1067 inspired synthetic three-dimensional model for pancreatic ductal adenocarcinoma
1068 organoids. *Nat. Mater.* <https://doi.org/10.1038/s41563-021-01085-1>
- 1069 Benton, G., Arnaoutova, I., George, J., Kleinman, H.K., Koblinski, J., 2014. Matrigel : From
1070 discovery and ECM mimicry to assays and models for cancer research. *Adv. Drug*
1071 *Deliv. Rev.* 79–80, 3–18. <https://doi.org/10.1016/j.addr.2014.06.005>
- 1072 Blanco-Fernandez, B., Gaspar, V.M., Engel, E., Mano, J.F., 2021. Proteinaceous Hydrogels
1073 for Bioengineering Advanced 3D Tumor Models. *Adv. Sci.* 8, 2003129.
- 1074 Brancato, V., Comunanza, V., Imperato, G., Corà, D., Urciuolo, F., Noghero, A., Bussolino,
1075 F., Netti, P.A., 2017. Bioengineered tumoral microtissues recapitulate desmoplastic
1076 reaction of pancreatic cancer. *Acta Biomater.* 49, 152–166.
1077 <https://doi.org/10.1016/j.actbio.2016.11.072>
- 1078 Broekgaarden, M., Anbil, S., Bulin, A.L., Obaid, G., Mai, Z., Baglo, Y., Rizvi, I., Hasan, T.,
1079 2019. Modulation of redox metabolism negates cancer-associated fibroblasts-induced
1080 treatment resistance in a heterotypic 3D culture platform of pancreatic cancer.
1081 *Biomaterials* 222, 119421. <https://doi.org/10.1016/j.biomaterials.2019.119421>
- 1082 Bulle, A., Lim, K.H., 2020. Beyond just a tight fortress: contribution of stroma to epithelial-
1083 mesenchymal transition in pancreatic cancer. *Signal Transduct. Target. Ther.* 5.
1084 <https://doi.org/10.1038/s41392-020-00341-1>
- 1085 Bynigeri, R.R., Jakkampudi, A., Jangala, R., Subramanyam, C., Sasikala, M., Rao, G.V.,
1086 Reddy, D.N., Talukdar, R., Bynigeri, R.R., Jakkampudi, A., Jangala, R., 2017.
1087 Pancreatic stellate cell : Pandora ' s box for pancreatic disease biology. *World J*
1088 *Gastroenterol* 23, 382–405. <https://doi.org/10.3748/wjg.v23.i3.382>
- 1089 Cao, X., Ashfaq, R., Cheng, F., 2019a. A Tumor-on-a-Chip System with Bioprinted Blood
1090 and Lymphatic Vessel Pair. <https://doi.org/10.1002/adfm.201970217>

- 1091 Cao, X., Ashfaq, R., Cheng, F., Maharjan, S., Li, J., Ying, G., Hassan, S., Xiao, H., Yue, K.,
 1092 Zhang, Y.S., 2019b. A Tumor-on-a-Chip System with Bioprinted Blood and Lymphatic
 1093 Vessel Pair. *Adv. Funct. Mater.* 29, 1807173. <https://doi.org/10.1002/adfm.201807173>
- 1094 Carvalho, M.R., Lima, D., Reis, R.L., Correlo, V.M., Oliveira, J.M., 2015. Evaluating
 1095 Biomaterial- and Microfluidic-Based 3D Tumor Models. *Trends Biotechnol.* 33, 667–
 1096 678. <https://doi.org/10.1016/j.tibtech.2015.09.009>
- 1097 Chang, C.Y., Lin, C.C., 2021. Hydrogel models with stiffness gradients for interrogating
 1098 pancreatic cancer cell fate. *Bioengineering* 8, 1–18.
 1099 <https://doi.org/10.3390/bioengineering8030037>
- 1100 Chang, Q., Ornatsky, O.I., Siddiqui, I., Loboda, A., Baranov, V.I., Hedley, D.W., 2017.
 1101 Imaging Mass Cytometry. *Cytom. Part A* 91A, 160–169.
 1102 <https://doi.org/10.1002/cyto.a.23053>
- 1103 Chen, K., Wang, Q., Li, M., Guo, H., Liu, W., Wang, F., Tian, X., Yang, Y., 2021. Single-
 1104 cell RNA-seq reveals dynamic change in tumor microenvironment during pancreatic
 1105 ductal adenocarcinoma malignant progression. *EBioMedicine* 66, 103315.
 1106 <https://doi.org/10.1016/j.ebiom.2021.103315>
- 1107 Chronopoulos, A., Lieberthal, T.J., del Río Hernández, A.E., 2017. Pancreatic cancer: a
 1108 mechanobiology approach. *Converg. Sci. Phys. Oncol.* 3. <https://doi.org/10.1088/2057-1739/aa5d1b>
- 1110 Costa, E.C., Moreira, A.F., de Melo-Diogo, D., Gaspar, V.M., Carvalho, M.P., Correia, I.J.,
 1111 2016. 3D tumor spheroids: an overview on the tools and techniques used for their
 1112 analysis. *Biotechnol. Adv.* 34, 1427–1441.
 1113 <https://doi.org/10.1016/j.biotechadv.2016.11.002>
- 1114 Daniel, S.K., Sullivan, K.M., Labadie, K.P., Pillarisetty, V.G., 2019. Hypoxia as a barrier to
 1115 immunotherapy in pancreatic adenocarcinoma. *Clin. Transl. Med.* 8.
 1116 <https://doi.org/10.1186/s40169-019-0226-9>
- 1117 Datta, P., Barui, A., Wu, Y., Ozbolat, V., Moncal, K.K., Ozbolat, I.T., 2018. Essential steps
 1118 in bioprinting: From pre- to post-bioprinting. *Biotechnol. Adv.* 36, 1481–1504.
 1119 <https://doi.org/10.1016/j.biotechadv.2018.06.003>
- 1120 Drifka, C.R., Eliceiri, K.W., Weber, S.M., Kao, W.J., 2013. A bioengineered heterotypic
 1121 stroma-cancer microenvironment model to study pancreatic ductal adenocarcinoma.
 1122 *Lab Chip* 13, 3965–3975. <https://doi.org/10.1039/c3lc50487e>
- 1123 Drost, J., Clevers, H., 2018. Organoids in cancer research. *Nat. Rev. Cancer* 18, 407–418.
 1124 <https://doi.org/10.1038/s41568-018-0007-6>
- 1125 Duchamp, M., Liu, T., van Genderen, A.M., Kappings, V., Oklu, R., Ellisen, L.W., Zhang,
 1126 Y.S., 2019. Sacrificial Bioprinting of a Mammary Ductal Carcinoma Model.
 1127 *Biotechnol. J.* 14, 1–9. <https://doi.org/10.1002/biot.201700703>
- 1128 Elyada, E., Bolisetty, M., Laise, P., Flynn, W.F., Elise, T., Burkhart, R.A., Teinor, J.A.,
 1129 Belleau, P., Biffi, G., Lucito, M.S., Sivajothi, S., Armstrong, T.D., Engle, D.D., Yu,
 1130 K.H., Hao, Y., Wolfgang, C.L., Park, Y., Preall, J., 2020. Cross-species single-cell
 1131 analysis of pancreatic ductal adenocarcinoma reveals antigen-presenting cancer-
 1132 associated fibroblasts. *Cancer Discov.* 9, 1102–1123. <https://doi.org/10.1158/2159-8290.CD-19-0094>
- 1134 Erdogan, B., Webb, D.J., 2017. Cancer-associated fibroblasts modulate growth factor
 1135 signaling and extracellular matrix remodeling to regulate tumor metastasis. *Biochem
 1136 Soc Trans* 45, 229–236. <https://doi.org/10.1042/BST20160387>
- 1137 Fang, Y., Eglén, R.M., 2017. Three-Dimensional Cell Cultures in Drug Discovery and
 1138 Development. *3D Cell Cult. Drug Screening, Optim. Three-Dimensional* 22, 456–472.

- 1139 Feig, C., Gopinathan, A., Neesse, A., Chan, D.S., Cook, N., Tuveson, D.A., 2012. The
 1140 pancreas cancer microenvironment. *Clin. Cancer Res.* 18, 4266–4276.
 1141 <https://doi.org/10.1158/1078-0432.CCR-11-3114>
- 1142 Ferdek, P.E., Jakubowska, M.A., 2017. Biology of pancreatic stellate cells — more than just
 1143 pancreatic cancer. *Pflugers Arch.* 469, 1039–1050. <https://doi.org/10.1007/s00424-017-1968-0>
- 1145 Ferreira, L.P., Gaspar, V.M., Mano, J.F., 2020. Decellularized Extracellular Matrix for
 1146 Bioengineering Physiomimetic 3D in Vitro Tumor Models. *Trends Biotechnol.* 38, 1–
 1147 18. <https://doi.org/10.1016/j.tibtech.2020.04.006>
- 1148 Ferreira, L.P., Gaspar, V.M., Mano, J.F., 2018. Design of spherically structured 3D in vitro
 1149 tumor models -Advances and prospects. *Acta Biomater.* 75, 11–34.
 1150 <https://doi.org/10.1016/j.actbio.2018.05.034>
- 1151 Ferreira, L.P., Gaspar, V.M., Monteiro, M. V., Freitas, B., Silva, N.J.O., Mano, J.F., 2021.
 1152 Screening of dual chemo-photothermal cellular nanotherapies in organotypic breast
 1153 cancer 3D spheroids. *J. Control. Release* 331, 85–102.
 1154 <https://doi.org/10.1016/j.jconrel.2020.12.054>
- 1155 Fiorini, E., Veghini, L., Corbo, V., 2020. Modeling Cell Communication in Cancer With
 1156 Organoids: Making the Complex Simple. *Front. Cell Dev. Biol.* 8, 1–12.
 1157 <https://doi.org/10.3389/fcell.2020.00166>
- 1158 Gaspar, V.M., Lavrador, P., Borges, J., Oliveira, M.B., Mano, J.F., 2019. Advanced Bottom-
 1159 Up Engineering of Living Architectures. *Adv. Mater.* 32, 1903975.
- 1160 Gaviraghi, M., Tunici, P., Valensin, S., Rossi, M., Giordano, C., Magnoni, L., Dandrea, M.,
 1161 Montagna, L., Ritelli, R., Scarpa, A., Bakker, A., 2011. Pancreatic cancer spheres are
 1162 more than just aggregates of stem marker-positive cells. *Biosci. Rep.* 31, 45–55.
 1163 <https://doi.org/10.1042/BSR20100018>
- 1164 Granat, L.M., Kambhampati, O., Klosek, S., Niedzwecki, B., Parsa, K., Zhang, D., 2019.
 1165 The promises and challenges of patient-derived tumor organoids in drug development
 1166 and precision oncology. *Anim. Model. Exp. Med.* 2, 150–161.
 1167 <https://doi.org/10.1002/ame2.12077>
- 1168 Grünwald, B.T., Devisme, A., Andrieux, G., Vyas, F., Aliar, K., Mccloskey, C.W., Macklin,
 1169 A., Jang, G.H., Denroche, R., Romero, J.M., Bavi, P., Bronsert, P., Notta, F., O’kane,
 1170 G., Wilson, J., Knox, J., Tamblyn, L., Radulovich, N., Fischer, S.E., Boerries, M.,
 1171 Gallinger, S., Kislinger, T., Khokha, R., Margaret, P., 2021. Spatially confined sub-
 1172 tumor microenvironments orchestrate pancreatic cancer pathobiology. *bioRxiv.*
 1173 <https://doi.org/10.1101/2021.02.18.431890>
- 1174 Guimarães, C.F., Gasperini, L., Marques, A.P., Reis, R.L., 2020. The stiffness of living
 1175 tissues and its implications for tissue engineering. *Nat. Rev. Mater.* 5, 351–370.
 1176 <https://doi.org/10.1038/s41578-019-0169-1>
- 1177 Hachey, S., Hughes, C., 2018. Applications of Tumor Chip Technology. *Lab Chip* 18, 2893–
 1178 2912.
- 1179 Hakobyan, D., Médina, C., Dusserre, N., Stachowicz, M.L., Handschin, C., Fricain, J.C.,
 1180 Guillermet-Guibert, J., Oliveira, H., 2020. Laser-assisted 3D bioprinting of exocrine
 1181 pancreas spheroid models for cancer initiation study. *Biofabrication* 12, 0–29.
 1182 <https://doi.org/10.1088/1758-5090/ab7cb8>
- 1183 Han, C., Liu, T., Yin, R., 2020. Biomarkers for cancer-associated fibroblasts. *Biomark. Res.*
 1184 8, 1–8. <https://doi.org/10.1186/s40364-020-00245-w>
- 1185 Ho, W.J., Jaffee, E.M., Zheng, L., 2020. The tumour microenvironment in pancreatic cancer
 1186 — clinical challenges and opportunities. *Nat. Rev. Clin. Oncol.* 17, 527–540.

1187 <https://doi.org/10.1038/s41571-020-0363-5>

1188 Hosein, A.N., Brekken, R.A., Maitra, A., 2020. Pancreatic cancer stroma: an update on
1189 therapeutic targeting strategies. *Nat. Rev. Gastroenterol. Hepatol.* 17, 487–505.
1190 <https://doi.org/10.1038/s41575-020-0300-1>

1191 Huang, L., Holtzinger, A., Jagan, I., BeGora, M., Lohse, I., Ngai, N., Nostro, C., Wang, R.,
1192 Muthuswamy, L.B., Crawford, H.C., Arrowsmith, C., Kalloger, S.E., Renouf, D.J.,
1193 Connor, A.A., Cleary, S., Schaeffer, D.F., Roehrl, M., Tsao, M.-S., Gallinger, S.,
1194 Keller, G., Muthuswamy, S.K., 2015. Ductal pancreatic cancer modeling and drug
1195 screening using human pluripotent stem cell and patient-derived tumor organoids. *Nat.*
1196 *Med.* 21, 1364–1371. <https://doi.org/10.1038/nm.3973>.

1197 Huang, W., Navarro-Serer, B., Jeong, Y.J., Chianchiano, P., Xia, L., Luchini, C., Veronese,
1198 N., Dowiak, C., Ng, T., Trujillo, M.A., Huang, B., Pflüger, M.J., Macgregor-Das, A.M.,
1199 Lionheart, G., Jones, D., Fujikura, K., Nguyen-Ngoc, K.-V., Neumann, N.M., Groot,
1200 V.P., Hasanain, A., van Oosten, A.F., Fischer, S.E., Gallinger, S., Singhi, A.D.,
1201 Zureikat, A.H., Brand, R.E., Gaida, M.M., Heinrich, S., Burkhart, R.A., He, J.,
1202 Wolfgang, C.L., Goggins, M.G., Thompson, E.D., Roberts, N.J., Ewald, A.J., Wood,
1203 L.D., 2020. Pattern of invasion in human pancreatic cancer organoids is associated with
1204 loss of SMAD4 and clinical outcome. *Cancer Res.* [https://doi.org/10.1158/0008-](https://doi.org/10.1158/0008-5472.can-19-1523)
1205 [5472.can-19-1523](https://doi.org/10.1158/0008-5472.can-19-1523)

1206 Hughes, C.S., Postovit, L.M., Lajoie, G.A., 2010. Matrigel: a complex protein mixture
1207 required for optimal growth of cell culture. *Proteomics* 10, 1886–1890.

1208 Itoh, Y., Takehara, Y., Kawase, T., Terashima, K., Ohkawa, Y., Hirose, Y., Koda, A.,
1209 Hyodo, N., Ushio, T., Hirai, Y., Yoshizawa, N., Yamashita, S., Nasu, H., Ohishi, N.,
1210 Sakahara, H., 2016. Feasibility of magnetic resonance elastography for the pancreas at
1211 3T. *J. Magn. Reson. Imaging* 43, 384–390. <https://doi.org/10.1002/jmri.24995>

1212 Jiang, B., Zhou, L., Lu, J., Wang, Y., Liu, C., You, L., Guo, J., 2020. Stroma-Targeting
1213 Therapy in Pancreatic Cancer: One Coin With Two Sides? *Front. Oncol.* 10, 1–9.
1214 <https://doi.org/10.3389/fonc.2020.576399>

1215 Karamitopoulou, E., 2019. Tumour microenvironment of pancreatic cancer: immune
1216 landscape is dictated by molecular and histopathological features. *Br. J. Cancer* 121, 5–
1217 14. <https://doi.org/10.1038/s41416-019-0479-5>

1218 Kiemen, A., Braxton, A.M., Grahn, M.P., Han, K.S., Babu, J.M., Reichel, R., Amoa, F.,
1219 Hong, S.M., Cornish, T.C., Thompson, E.D., Wood, L.D., Hruban, R.H., Wu, P.H.,
1220 Wirtz, D., 2020. In situ characterization of the 3D microanatomy of the pancreas and
1221 pancreatic cancer at single cell resolution. *bioRxiv* 2020.12.08.416909.

1222 Kim, P.K., Halbrook, C.J., Kerk, S.A., Wisner, S., (...), Lyssiotis, C.A., 2020. Hyaluronic
1223 Acid Fuels Pancreatic Cancer Growth. *bioRxiv*.

1224 Kleeff, J., Beckhove, P., Esposito, I., Herzig, S., Huber, P.E., Löhr, J.M., Friess, H., 2007.
1225 Pancreatic cancer microenvironment. *Int. J. Cancer* 121, 699–705.
1226 <https://doi.org/10.1002/ijc.22871>

1227 Kleeff, J., Korc, M., Apte, M., La Vecchia, C., Johnson, C.D., Biankin, A. V, Neale, R.E.,
1228 Tempero, M., Tuveson, D.A., Hruban, R.H., Neoptolemos, J.P., 2016. Pancreatic
1229 cancer. *Nat. Rev. Dis. Prim.* 2, 16022. <https://doi.org/10.1038/nrdp.2016.22>

1230 Knudsen, E.S., Balaji, U., Freinkman, E., Mccue, P., 2016. Unique metabolic features of
1231 pancreatic cancer stroma: relevance to the tumor compartment , prognosis , and
1232 invasive potential. *Oncotarget* 7, 78396–78411.

1233 Koikawa, K., Ohuchida, K., Ando, Y., Kibe, S., Nakayama, H., Takesue, S., Endo, S., Abe,
1234 T., Okumura, T., Iwamoto, C., Moriyama, T., Nakata, K., Miyasaka, Y., Ohtsuka, T.,

1235 Nagai, E., Mizumoto, K., Hashizume, M., Nakamura, M., 2018. Basement membrane
1236 destruction by pancreatic stellate cells leads to local invasion in pancreatic ductal
1237 adenocarcinoma. *Cancer Lett.* 425, 65–77. <https://doi.org/10.1016/j.canlet.2018.03.031>

1238 Kolipaka, A., Schroeder, S., Mo, X., Shah, Z., Hart, P.A., Conwell, D.L., 2017. Magnetic
1239 resonance elastography of the pancreas: Measurement reproducibility and relationship
1240 with age. *Magn. Reson. Imaging* 42, 1–7. <https://doi.org/10.1016/j.mri.2017.04.015>

1241 Kota, J., Hancock, J., Kwon, J., Korc, M., 2017. Pancreatic cancer: Stroma and its current
1242 and emerging targeted therapies. *Cancer Lett.* 391, 38–49.
1243 <https://doi.org/10.1016/j.canlet.2016.12.035>

1244 Kuen, J., Darowski, D., Kluge, T., Majety, M., 2017. Pancreatic cancer cell/fibroblast co-
1245 culture induces M2 like macrophages that influence therapeutic response in a 3D model.
1246 *PLoS One* 12, 1–19. <https://doi.org/10.1371/journal.pone.0182039>

1247 Lai, B.F.L., Lu, R.X.Z., Hu, Y., Davenport Huyer, L., Dou, W., Wang, E.Y., Radulovich,
1248 N., Tsao, M.S., Sun, Y., Radisic, M., 2020. Recapitulating Pancreatic Tumor
1249 Microenvironment through Synergistic Use of Patient Organoids and Organ-on-a-Chip
1250 Vasculature. *Adv. Funct. Mater.* 30, 1–16. <https://doi.org/10.1002/adfm.202000545>

1251 Langer, E.M., Allen-Petersen, B.L., King, S.M., Kendsersky, N.D., Turnidge, M.A., Kuziel,
1252 G.M., Riggers, R., Samatham, R., Amery, T.S., Jacques, S.L., Sheppard, B.C., Korkola,
1253 J.E., Muschler, J.L., Thibault, G., Chang, Y.H., Gray, J.W., Presnell, S.C., Nguyen,
1254 D.G., Sears, R.C., 2019. Modeling Tumor Phenotypes In Vitro with Three-Dimensional
1255 Bioprinting. *Cell Rep.* 26, 608–623.e6. <https://doi.org/10.1016/j.celrep.2018.12.090>

1256 Lankadasari, M.B., Mukhopadhyay, P., Mohammed, S., Harikumar, K.B., 2019. TAMing
1257 pancreatic cancer: Combat with a double edged sword. *Mol. Cancer* 18, 1–13.
1258 <https://doi.org/10.1186/s12943-019-0966-6>

1259 Laschke, M.W., Menger, M.D., 2017. Life is 3D: Boosting Spheroid Function for Tissue
1260 Engineering. *Trends Biotechnol.* 35, 133–144.
1261 <https://doi.org/10.1016/j.tibtech.2016.08.004>

1262 Lazzari, G., Nicolas, V., Matsusaki, M., Akashi, M., Couvreur, P., Mura, S., 2018.
1263 Multicellular spheroid based on a triple co-culture: A novel 3D model to mimic
1264 pancreatic tumor complexity. *Acta Biomater.* 78, 296–307.
1265 <https://doi.org/10.1016/j.actbio.2018.08.008>

1266 Li, Y., Zhang, T., Pang, Y., Li, L., Chen, Z.N., Sun, W., 2019. 3D bioprinting of hepatoma
1267 cells and application with microfluidics for pharmacodynamic test of Metuzumab.
1268 *Biofabrication* 11, 34102. <https://doi.org/10.1088/1758-5090/ab256c>

1269 Liaw, C.Y., Ji, S., Guvendiren, M., 2018. Engineering 3D Hydrogels for Personalized In
1270 Vitro Human Tissue Models. *Adv. Healthc. Mater.* 7, 1701165.
1271 <https://doi.org/10.1002/adhm.201701165>

1272 Lin, C.C., Korc, M., 2018. Designer hydrogels: Shedding light on the physical chemistry of
1273 the pancreatic cancer microenvironment. *Cancer Lett.* 436, 22–27.
1274 <https://doi.org/10.1016/j.canlet.2018.08.008>

1275 Lin, M., Gao, M., Pandalai, P.K., Cavnar, M.J., Kim, J., 2020. An organotypic microcosm
1276 for the pancreatic tumor microenvironment. *Cancers (Basel)*. 12, 1–12.
1277 <https://doi.org/10.3390/cancers12040811>

1278 Lin, W., Noel, P., Borazanci, E.H., Lee, J., Amini, A., Han, I.W., Heo, J.S., Jameson, G.S.,
1279 Fraser, C., Steinbach, M., Woo, Y., Fong, Y., Cridebring, D., Hoff, D.D. Von, Park,
1280 J.O., Han, H., 2020. Single-cell transcriptome analysis of tumor and stromal
1281 compartments of pancreatic ductal adenocarcinoma primary tumors and metastatic
1282 lesions. *Genome Med.* 1–14. <https://doi.org/10.1186/s13073-020-00776-9>

1283 Liot, S., Balas, J., Aubert, A., Prigent, L., Mercier-Gouy, P., Verrier, B., Bertolino, P.,
1284 Hennino, A., Valcourt, U., Lambert, E., 2021. Stroma Involvement in Pancreatic Ductal
1285 Adenocarcinoma: An Overview Focusing on Extracellular Matrix Proteins. *Front.*
1286 *Immunol.* 12, 1–12. <https://doi.org/10.3389/fimmu.2021.612271>

1287 Little, A.C., Kovalenko, I., Goo, L.E., Hong, H.S., Kerk, S.A., Yates, J.A., Purohit, V.,
1288 Lombard, D.B., Lyssiotis, C.A., 2020. High-content fluorescence imaging with the
1289 metabolic flux assay reveals insights into mitochondrial properties and functions.
1290 *Commun. Biol.* 1–10. <https://doi.org/10.1038/s42003-020-0988-z>

1291 Liu, H.Y., Greene, T., Lin, T.Y., Dawes, C.S., Korc, M., Lin, C.C., 2017. Enzyme-mediated
1292 stiffening hydrogels for probing activation of pancreatic stellate cells. *Acta Biomater.*
1293 48, 258–269. <https://doi.org/10.1016/j.actbio.2016.10.027>

1294 Liu, H.Y., Korc, M., Lin, C.C., 2018. Biomimetic and enzyme-responsive dynamic
1295 hydrogels for studying cell-matrix interactions in pancreatic ductal adenocarcinoma.
1296 *Biomaterials* 160, 24–36. <https://doi.org/10.1016/j.biomaterials.2018.01.012>

1297 Liu, X., Zheng, W., Wang, W., Shen, H., Liu, L., Lou, W., Wang, X., Yang, P., 2017. A new
1298 panel of pancreatic cancer biomarkers discovered using a mass spectrometry-based
1299 pipeline. *Br. J. Cancer* 117, 1846–1854. <https://doi.org/10.1038/bjc.2017.365>

1300 Luo, G., Long, J., Zhang, B., Liu, C., Xu, J., Ni, Q., Yu, X., 2012. Stroma and pancreatic
1301 ductal adenocarcinoma: An interaction loop. *Biochim. Biophys. Acta - Rev. Cancer*
1302 1826, 170–178. <https://doi.org/10.1016/j.bbcan.2012.04.002>

1303 Ma, X., Yu, C., Wang, P., Xu, W., Wan, X., Lai, C.S.E., Liu, J., Koroleva-Maharajh, A.,
1304 Chen, S., 2018. Rapid 3D bioprinting of decellularized extracellular matrix with
1305 regionally varied mechanical properties and biomimetic microarchitecture.
1306 *Biomaterials* 185, 310–321. <https://doi.org/10.1016/j.biomaterials.2018.09.026>

1307 Makohon-Moore, A., Iacobuzio-Donahue, C.A., 2016. Pancreatic cancer biology and
1308 genetics from an evolutionary perspective. *Nat. Rev. Cancer* 16, 553–565.
1309 <https://doi.org/10.1038/nrc.2016.66>

1310 Mantovani, A., Marchesi, F., Malesci, A., Laghi, L., Allavena, P., 2017. Tumour-associated
1311 macrophages as treatment targets in oncology. *Nat. Rev. Clin. Oncol.* 14, 399–416.
1312 <https://doi.org/10.1038/nrclinonc.2016.217>

1313 McCarroll, J.A., Naim, S., Sharbeen, G., Russia, N., Lee, J., Kavallaris, M., Goldstein, D.,
1314 Phillips, P.A., 2014. Role of pancreatic stellate cells in chemoresistance in pancreatic
1315 cancer. *Front. Physiol.* 5, 1–9. <https://doi.org/10.3389/fphys.2014.00141>

1316 Monteiro, C.F., Santos, S.C., Custódio, C.A., Mano, J.F., 2020. Human Platelet Lysates-
1317 Based Hydrogels: A Novel Personalized 3D Platform for Spheroid Invasion
1318 Assessment. *Adv. Sci.* 7, 1902398. <https://doi.org/10.1002/advs.201902398>

1319 Monteiro, M. V., Gaspar, V.M., Ferreira, L.P., Mano, J.F., 2020a. Hydrogel 3D: In vitro
1320 tumor models for screening cell aggregation mediated drug response. *Biomater. Sci.* 8,
1321 1855–1864. <https://doi.org/10.1039/c9bm02075f>

1322 Monteiro, M. V., Gaspar, V.M., Mano, J.F., 2020b. Chapter 2 - Bioinspired biomaterials to
1323 develop cell-rich spherical microtissues for 3D in vitro tumor modeling, in:
1324 *Biomaterials for 3D Tumor Modeling*. pp. 43–65. <https://doi.org/10.1016/B978-0-12-818128-7.00002-2>

1325
1326 Monteiro, M. V., Gaspar, V.M., Mendes, L., Duarte, I.F., Mano, J.F., 2021a. Stratified 3D
1327 Microtumors as Organotypic Testing Platforms for Screening Pancreatic Cancer
1328 Therapies. *Small Methods* 5, 2001207.

1329 Monteiro, M. V., Zhang, Y.S., Gaspar, V.M., Mano, J.F., 2021b. 3D-bioprinted cancer-on-a-
1330 chip: level-up organotypic in vitro models. *Trends Biotechnol.*

- 1331 Murakami, T., Hiroshima, Y., Matsuyama, R., Homma, Y., Hoffman, R.M., Endo, I., 2019.
1332 Role of the tumor microenvironment in pancreatic cancer. *Ann. Gastroenterol. Surg.* 3,
1333 130–137. <https://doi.org/10.1002/ags3.12225>
- 1334 Nabavizadeh, A., Payen, T., Iuga, A.C., Sagalovskiy, I.R., Desrouilleres, D., Saharkhiz, N.,
1335 Palermo, C.F., Sastra, S.A., Oberstein, P.E., Rosario, V., Kluger, M.D., Schrope, B.A.,
1336 Chabot, J.A., Olive, K.P., Konofagou, E.E., 2020. Noninvasive Young's modulus
1337 visualization of fibrosis progression and delineation of pancreatic ductal
1338 adenocarcinoma (PDAC) tumors using Harmonic Motion Elastography (HME) in vivo.
1339 *Theranostics* 10, 4614–4626. <https://doi.org/10.7150/thno.37965>
- 1340 Nabavizadeh, A., Payen, T., Saharkhiz, N., McGarry, M., Olive, K.P., Konofagou, E.E.,
1341 2018. Technical Note: In vivo Young's modulus mapping of pancreatic ductal
1342 adenocarcinoma during HIFU ablation using harmonic motion elastography (HME).
1343 *Med. Phys.* 45, 5244–5250. <https://doi.org/10.1002/mp.13170>
- 1344 Nagle, P.W., Plukker, J.T.M., Muijs, C.T., van Luijk, P., Coppes, R.P., 2018. Patient-derived
1345 tumor organoids for prediction of cancer treatment response. *Semin. Cancer Biol.* 53,
1346 258–264. <https://doi.org/10.1016/j.semcancer.2018.06.005>
- 1347 Nguyen, D.H.T., Lee, E., Alimperti, S., Norgard, R.J., Wong, A., Lee, J.J.K., Eyckmans, J.,
1348 Stanger, B.Z., Chen, C.S., 2019. A biomimetic pancreatic cancer on-chip reveals
1349 endothelial ablation via ALK7 signaling. *Sci. Adv.* 5, 1–10.
1350 <https://doi.org/10.1126/sciadv.aav6789>
- 1351 Nguyen, A. V., Nyberg, K.D., Scott, M.B., Welsh, A.M., Nguyen, A.H., Wu, N., Hohlbauch,
1352 S. V., Geisse, N.A., Gibb, E.A., Robertson, A.G., Donahue, T.R., Rowat, A.C., 2016a.
1353 Stiffness of pancreatic cancer cells is associated with increased invasive potential.
1354 *Integr. Biol. (United Kingdom)* 8, 1232–1245. <https://doi.org/10.1039/c6ib00135a>
- 1355 Nguyen, A. V., Nyberg, K.D., Scott, M.B., Welsh, A.M., Nguyen, A.H., Wu, N., Hohlbauch,
1356 S. V., Geisse, N.A., Gibb, E.A., Robertson, A.G., Donahue, T.R., Rowat, A.C., 2016b.
1357 Stiffness of pancreatic cancer cells is associated with increased invasive potential.
1358 *Integr Biol* 8, 1232–1245. <https://doi.org/10.1039/c6ib00135a>
- 1359 Nia, H.T., Munn, L.L., Jain, R.K., 2020. Physical traits of cancer. *Science (80-.)*. 370, 6516.
1360 <https://doi.org/10.1126/SCIENCE.AAZ0868>
- 1361 Norton, J., Foster, D., Chinta, M., Titan, A., Longaker, M., 2020. Pancreatic cancer
1362 associated fibroblasts (CAF): Under-explored target for pancreatic cancer treatment.
1363 *Cancers (Basel)*. 12, 1–18. <https://doi.org/10.3390/cancers12051347>
- 1364 Olive, K.P., 2015. Stroma, stroma everywhere (Far more than you think). *Clin. Cancer Res.*
1365 21, 3366–3368. <https://doi.org/10.1158/1078-0432.CCR-15-0416>
- 1366 Orth, M., Metzger, P., Gerum, S., Mayerle, J., Schneider, G., Belka, C., Schnurr, M., Lauber,
1367 K., 2019. Pancreatic ductal adenocarcinoma: Biological hallmarks, current status, and
1368 future perspectives of combined modality treatment approaches. *Radiat. Oncol.* 14, 1–
1369 20. <https://doi.org/10.1186/s13014-019-1345-6>
- 1370 Pandol, S., Edderkaoui, M., Gukovsky, I., Lugea, A., Gukovskaya, A., 2009. Desmoplasia
1371 of Pancreatic Ductal Adenocarcinoma. *Clin. Gastroenterol. Hepatol.* 7, 1–9.
1372 <https://doi.org/10.1016/j.cgh.2009.07.039>
- 1373 Pathria, P., Louis, T.L., Varner, J.A., 2019. Targeting Tumor-Associated Macrophages in
1374 Cancer. *Trends Immunol.* 40, 310–327. <https://doi.org/10.1016/j.it.2019.02.003>
- 1375 Pereira, B.A., Vennin, C., Papanicolaou, M., Chambers, C.R., Herrmann, D., Morton, J.P.,
1376 Cox, T.R., Timpson, P., 2019. CAF Subpopulations: A New Reservoir of Stromal
1377 Targets in Pancreatic Cancer. *Trends in Cancer* 5, 724–741.
1378 <https://doi.org/10.1016/j.trecan.2019.09.010>

- 1379 Pereira, R.F., Bártolo, P.J., 2015. 3D Printing — Review 3D Photo-Fabrication for Tissue
1380 Engineering and Drug. Engineering 1, 90–112.
- 1381 Pinto, M.L., Rios, E., Silva, A.C., Neves, S.C., Caires, H.R., Pinto, A.T., Durães, C.,
1382 Carvalho, F.A., Cardoso, A.P., Santos, N.C., Barrias, C.C., Nascimento, D.S., Pinto-
1383 do-Ó, P., Barbosa, M.A., Carneiro, F., Oliveira, M.J., 2017. Decellularized human
1384 colorectal cancer matrices polarize macrophages towards an anti-inflammatory
1385 phenotype promoting cancer cell invasion via CCL18. Biomaterials 124, 211–224.
1386 <https://doi.org/10.1016/j.biomaterials.2017.02.004>
- 1387 Pothula, S.P., Pirola, R.C., Wilson, J.S., Apte, M. V., 2020. Pancreatic stellate cells: Aiding
1388 and abetting pancreatic cancer progression. Pancreatology 20, 409–418.
1389 <https://doi.org/10.1016/j.pan.2020.01.003>
- 1390 Pradhan, S., Clary, J.M., Seliktar, D., Lipke, E.A., 2017. A three-dimensional spheroidal
1391 cancer model based on PEG-fibrinogen hydrogel microspheres. Biomaterials 115, 141–
1392 154. <https://doi.org/10.1016/j.biomaterials.2016.10.052>
- 1393 Puls, T.J., Tan, X., Husain, M., Whittington, C.F., Fishel, M.L., Voytik-Harbin, S.L., 2018.
1394 Development of a Novel 3D Tumor-tissue Invasion Model for High-throughput, High-
1395 content Phenotypic Drug Screening. Sci. Rep. 8, 1–14. <https://doi.org/10.1038/s41598-018-31138-6>
- 1397 Rebelo, S.P., Pinto, C., Martins, T.R., Harrer, N., Estrada, M.F., Loza-Alvarez, P.,
1398 Cabeçadas, J., Alves, P.M., Gualda, E.J., Sommergruber, W., Brito, C., 2018. 3D-3-
1399 culture: A tool to unveil macrophage plasticity in the tumour microenvironment.
1400 Biomaterials 163, 185–197.
- 1401 Reid, J.A., Palmer, X., Peter, A.M., Northam, N., Sachs, P.C., Bruno, R.D., 2019. A 3D
1402 bioprinter platform for mechanistic analysis of tumoroids and chimeric mammary
1403 organoids. Sci. Rep. 9, 1–10. <https://doi.org/10.1038/s41598-019-43922-z>
- 1404 Ricci, C., Mota, C., Moscato, S., D’Alessandro, D., Ugel, S., Sartoris, S., Bronte, V., Boggi,
1405 U., Campani, D., Funel, N., Moroni, L., Danti, S., 2014. Interfacing polymeric scaffolds
1406 with primary pancreatic ductal adenocarcinoma cells to develop 3D cancer models.
1407 Biomatter 4. <https://doi.org/10.4161/21592527.2014.955386>
- 1408 Rice, A.J., Cortes, E., Lachowski, D., Cheung, B.C.H., Karim, S.A., Morton, J.P., del Río
1409 Hernández, A., 2017. Matrix stiffness induces epithelial–mesenchymal transition and
1410 promotes chemoresistance in pancreatic cancer cells. Oncogenesis 6, e352–e352.
1411 <https://doi.org/10.1038/oncsis.2017.54>
- 1412 Rubiano, A., Delitto, D., Han, S., Gerber, M., Galitz, C., Trevino, J., Thomas, R.M., Hughes,
1413 S.J., Simmons, C.S., 2018. Viscoelastic properties of human pancreatic tumors and in
1414 vitro constructs to mimic mechanical properties. Acta Biomater. 67, 331–340.
1415 <https://doi.org/10.1016/j.actbio.2017.11.037>
- 1416 Sahai, E., Astsaturov, I., Cukierman, E., Denardo, D.G., Egeblad, M., Evans, R.M., Fearon,
1417 D., Greten, F.R., Hingorani, S.R., Hunter, T., Hynes, R.O., Jain, R.K., Janowitz, T.,
1418 Jorgensen, C., Kimmelman, A.C., Kolonin, M.G., Maki, R.G., Powers, R.S., Puré, E.,
1419 Ramirez, D.C., Scherz-shouval, R., Sherman, M.H., Stewart, S., Tlsty, T.D., Tuveson,
1420 D.A., Watt, F.M., Weaver, V., Weeraratna, A.T., Werb, Z., 2020. A framework for
1421 advancing our understanding of cancer- associated fibroblasts. Nat. Rev. Cancer 20,
1422 174–186. <https://doi.org/10.1038/s41568-019-0238-1>
- 1423 Santi, A., Kugeratski, F.G., Zanivan, S., 2017. Cancer Associated Fibroblasts: The
1424 Architects of Stroma Remodeling. Proteomics 18, e1700167.
- 1425 Sapudom, J., Müller, C.D., Nguyen, K., Martin, S., Ulf, A., Pompe, T., 2020. Matrix
1426 Remodeling and Hyaluronan Production by Myofibroblasts and Cancer-Associated

1427 Fibroblasts in 3D Collagen Matrices. gels 6.

1428 Sato, N., Kohi, S., Hirata, K., Goggins, M., 2016. Role of hyaluronan in pancreatic cancer
1429 biology and therapy: Once again in the spotlight. *Cancer Sci.* 107, 569–575.

1430 Sazeides, C., Le, A., 2018. Metabolic Relationship between Cancer- - Associated Fibroblasts
1431 and Cancer Cells, in: *Advances in Experimental Medicine and Biology.* pp. 149–165.
1432 <https://doi.org/10.1007/978-3-319-77736-8>

1433 Schnittert, J., Bansal, R., Prakash, J., 2019. Targeting Pancreatic Stellate Cells in Cancer.
1434 *TRENDS in CANCER* 5, 128–142. <https://doi.org/10.1016/j.trecan.2019.01.001>

1435 Shang, M., Soon, R.H., Lim, C.T., Khoo, B.L., Han, J., 2019. Microfluidic modelling of the
1436 tumor microenvironment for anti-cancer drug development. *Lab Chip* 19, 369–386.
1437 <https://doi.org/10.1039/c8lc00970h>

1438 Shi, Y., Cang, L., Zhang, X., Cai, X., Wang, X., Ji, R., Wang, M., Hong, Y., 2018. The use
1439 of magnetic resonance elastography in differentiating autoimmune pancreatitis from
1440 pancreatic ductal adenocarcinoma: a preliminary study. *Eur. J. Radiol.* 108, 13–20.

1441 Shih, H., Greene, T., Korc, M., Lin, C.C., 2016. Modular and Adaptable Tumor Niche
1442 Prepared from Visible Light Initiated Thiol-Norbornene Photopolymerization.
1443 *Biomacromolecules* 17, 3872–3882. <https://doi.org/10.1021/acs.biomac.6b00931>

1444 Steele, N.G., Carpenter, E.S., Kemp, S.B., Sirihorachai, V.R., The, S., Delrosario, L.,
1445 Lazarus, J., Amir, E.D., Gunchick, V., Espinoza, C., Bell, S., Harris, L., Lima, F.,
1446 Irizarry-negron, V., Paglia, D., Macchia, J., Ka, A., Chu, Y., Schofield, H., Wamsteker,
1447 E., Kwon, R., Schulman, A., Prabhu, A., Law, R., Sondhi, A., Yu, J., Patel, A.,
1448 Donahue, K., Nathan, H., Cho, C., Anderson, M.A., Sahai, V., Lyssiotis, C.A., Zou,
1449 W., Allen, B.L., Rao, A., Crawford, H.C., Bednar, F., Frankel, T.L., Pasca, M., 2020.
1450 Multimodal mapping of the tumor and peripheral blood immune landscape in human
1451 pancreatic cancer. *Nat. Cancer* 1, 1097–1112. <https://doi.org/10.1038/s43018-020-00121-4>

1452

1453 Stopa, K.B., Kusiak, A.A., Szopa, M.D., Ferdek, P.E., Jakubowska, M.A., 2020. Pancreatic
1454 cancer and its microenvironment—recent advances and current controversies. *Int. J.*
1455 *Mol. Sci.* 21. <https://doi.org/10.3390/ijms21093218>

1456 Sugimoto, M., Takahashi, S., Kojima, M., 2014. What is the nature of pancreatic
1457 consistency ? Assessment of the elastic modulus of the pancreas and comparison with
1458 tactile sensation , histology , and occurrence of postoperative pancreatic fistula after
1459 pancreaticoduodenectomy. *Surgery* 156, 1204–1211.
1460 <https://doi.org/10.1016/j.surg.2014.05.015>

1461 Suklabaidya, S., Dash, P., Das, B., Suresh, V., Sasmal, P.K., Senapati, S., 2018.
1462 Experimental models of pancreatic cancer desmoplasia. *Lab. Investig.* 98, 27–40.
1463 <https://doi.org/10.1038/labinvest.2017.127>

1464 Sun, Q., Zhang, B., Hu, Q., Qin, Y., Xu, W., Liu, W., Yu, X., Xu, J., 2018. The impact of
1465 cancer-associated fibroblasts on major hallmarks of pancreatic cancer. *Theranostics* 8,
1466 5072–5087. <https://doi.org/10.7150/thno.26546>

1467 Tanaka, H.Y., Kurihara, T., Nakazawa, T., Matsusaki, M., Masamune, A., Kano, M.R.,
1468 2020. Heterotypic 3D pancreatic cancer model with tunable proportion of fibrotic
1469 elements. *Biomaterials* 251, 120077.
1470 <https://doi.org/10.1016/j.biomaterials.2020.120077>

1471 Tian, C., Clauser, K.R., Öhlund, D., Rickelt, S., Huang, Y., Gupta, M., Mani, D.R., Carr,
1472 S.A., Tuveson, D.A., Hynes, R.O., 2019. Proteomic analyses of ECM during pancreatic
1473 ductal adenocarcinoma progression reveal different contributions by tumor and stromal
1474 cells. *Proc. Natl. Acad. Sci.* <https://doi.org/10.1073/pnas.1908626116>

- 1475 Tomás-Bort, E., Kieler, M., Sharma, S., Candido, J.B., Loessner, D., 2020. 3D approaches
1476 to model the tumor microenvironment of pancreatic cancer. *Theranostics* 10, 5074–
1477 5089. <https://doi.org/10.7150/thno.42441>
- 1478 Tsai, S., McOlash, L., Palen, K., Johnson, B., Duris, C., Yang, Q., Dwinell, M.B., Hunt, B.,
1479 Evans, D.B., Gershan, J., James, M.A., 2018. Development of primary human
1480 pancreatic cancer organoids, matched stromal and immune cells and 3D tumor
1481 microenvironment models. *BMC Cancer* 18, 1–13. <https://doi.org/10.1186/s12885-018-4238-4>
- 1482
- 1483 Wang, C., Tang, Z., Zhao, Y., Yao, R., Li, L., Sun, W., 2014. Three-dimensional in vitro
1484 cancer models: A short review. *Biofabrication* 6, 022001. <https://doi.org/10.1088/1758-5082/6/2/022001>
- 1485
- 1486 Wang, S., Li, Y., Xing, C., Ding, C., Zhang, H., Chen, L., You, L., Dai, M., Zhao, Y., 2020.
1487 Tumor microenvironment in chemoresistance, metastasis and immunotherapy of
1488 pancreatic cancer. *Am. J. Cancer Res.* 10, 1937–1953.
- 1489 Ware, M.J., Keshishian, V., Law, J.J., Ho, J.C., Favela, C.A., Rees, P., Smith, B.,
1490 Mohammad, S., Hwang, R.F., Rajapakshe, K., Coarfa, C., Huang, S., Edwards, D.P.,
1491 Corr, S.J., Godin, B., Curley, S.A., 2016. Generation of an in vitro 3D PDAC stroma
1492 rich spheroid model. *Biomaterials* 108, 129–142.
1493 <https://doi.org/10.1016/j.biomaterials.2016.08.041>
- 1494 Watt, J., Kocher, H.M., 2013. The desmoplastic stroma of pancreatic cancer is a barrier to
1495 immune cell infiltration. *Oncoimmunology* 2, 1–4. <https://doi.org/10.4161/onci.26788>
- 1496 Weniger, M., Honselmann, K.C., Liss, A.S., 2018. The Extracellular Matrix and Pancreatic
1497 Cancer: A Complex Relationship. *Cancers (Basel)*. 10, 316.
1498 <https://doi.org/10.3390/cancers10090316>
- 1499 Winkler, J., Abisoye-Ogunniyan, A., Metcalf, K.J., Werb, Z., 2020. Concepts of
1500 extracellular matrix remodelling in tumour progression and metastasis. *Nat. Commun.*
1501 11, 1–19. <https://doi.org/10.1038/s41467-020-18794-x>
- 1502 Wong, C.W., Han, H.W., Tien, Y.W., Hsu, S. hui, 2019. Biomaterial substrate-derived
1503 compact cellular spheroids mimicking the behavior of pancreatic cancer and
1504 microenvironment. *Biomaterials* 213, 1–15.
1505 <https://doi.org/10.1016/j.biomaterials.2019.05.013>
- 1506 Wörmann, S.M., Diakopoulos, K.N., Lesina, M., Algül, H., 2014. The immune network in
1507 pancreatic cancer development and progression. *Oncogene* 33, 2956–2967.
1508 <https://doi.org/10.1038/onc.2013.257>
- 1509 Xiang, X., Wang, J., Lu, D., Xu, X., 2021. Targeting tumor-associated macrophages to
1510 synergize tumor immunotherapy. *Signal Transduct. Target. Ther.* 6.
1511 <https://doi.org/10.1038/s41392-021-00484-9>
- 1512 Yang, S., Liu, Q., Liao, Q., 2021. Tumor-Associated Macrophages in Pancreatic Ductal
1513 Adenocarcinoma: Origin, Polarization, Function, and Reprogramming. *Front. Cell Dev.*
1514 *Biol.* 8, 1–24. <https://doi.org/10.3389/fcell.2020.607209>
- 1515 Yin, J., Yan, M., Wang, Y., Fu, J., Suo, H., 2018. 3D Bioprinting of Low-Concentration
1516 Cell-Laden Gelatin Methacrylate (GelMA) Bioinks with a Two-Step Cross-linking
1517 Strategy. *ACS Appl. Mater. Interfaces* 10, 6849–6857.
- 1518 Yoshikawa, M., Ishikawa, T., Ohno, E., Iida, T., Furukawa, K., Nakamura, M., Honda, T.,
1519 Ishigami, M., Kinoshita, F., Kawashima, H., Fujishiro, M., 2021. Variability
1520 measurements provide additional value to shear wave elastography in the diagnosis of
1521 pancreatic cancer. *Sci. Rep.* 11, 1–8. <https://doi.org/10.1038/s41598-021-86979-5>
- 1522 Yu, F., Choudhury, D., 2019. Microfluidic bioprinting for organ-on- a-chip models. *Drug*

1523 Discov. Today 24, 1248–1258. <https://doi.org/10.1016/j.drudis.2019.03.025>
1524 Zanutelli, M.R., Chada, N.C., Johnson, C.A., Reinhart-King, C.A., 2020. The Physical
1525 Microenvironment of Tumors: Characterization and Clinical Impact. *Biophys. Rev.*
1526 *Lett.* 15, 51–82. <https://doi.org/10.1142/s1793048020300029>
1527 Zhan, H. xiang, Zhou, B., Cheng, Y. gang, Xu, J. wei, Wang, L., Zhang, G. yong, Hu, S.
1528 yuan, 2017. Crosstalk between stromal cells and cancer cells in pancreatic cancer: New
1529 insights into stromal biology. *Cancer Lett.* 392, 83–93.
1530 <https://doi.org/10.1016/j.canlet.2017.01.041>
1531 Zhang, Y.S., Pi, Q., van Genderen, A.M., 2017. Microfluidic bioprinting for engineering
1532 vascularized tissues and organoids. *J. Vis. Exp.* 126, 1–8. <https://doi.org/10.3791/55957>
1533